Science and Technology for Energy Transition **79**, 39 (2024)

https://doi.org/10.2516/stet/2024037

Available online at:
stet-review.org

Decarbonizing Energy Systems: Smart Grid and Renewable Technologies
Fang Rui-ming and Qiangqiang Liao (Guest Editors)

REGULAR ARTICLE OPEN ACCESS

Integrating multiple vehicle drivetrains into an energy system simulation model for Japan

K. Knüpfer[1,*], N. Rogalski[2], A. Knüpfer[3], M. Esteban[1], and T. Shibayama[1]

[1] Department of Civil and Environmental Engineering, Waseda University, 4-1 Okubo 3, Shinjuku-ku, 169-8555 Tokyo, Japan
[2] Faculty of Medicine, Hamburg University, Martinistraße 52, Building N55, 20246 Hamburg, Germany
[3] SEAK Software GmbH, Röntgenstraße 31-33, 21465 Reinbek, Germany

Received: 6 February 2024 / Accepted: 23 May 2024

Abstract. To reduce the impact of climate change, the Japanese economy has set mitigation goals that include the decarbonisation of the energy sector and the electrification of transport. As a result, zero-emission vehicles could change the electricity demand curve, and it is thus necessary for them to be integrated into energy system models to estimate their impact and any opportunities or challenges they represent to grid stability. While previous studies have integrated single-vehicle technologies in the simulation of country-level energy grids, the present study improves on available models by integrating a country-level energy system model with a transmission grid, while considering two different drivetrains and improving on the diversity of the vehicle movement patterns considered. The simulation model results highlight that the electricity demand of each drivetrain is distinct, with a midday peak for battery electric vehicles and less pronounced morning and afternoon peaks for fuel cell electric vehicles. An important conclusion is that the infrastructure setup and associated use rules can be expected to significantly impact transport demand curves, indicating the need to further investigate how policy changes can impact the overall configuration of the energy mix.

Keywords: Electricity grid modelling, Renewable energy mix, Japan, Vehicles, BEV, FCEV.

1 Introduction

As a signee to the 2015 Paris Agreement [1], the Japanese government has published and revised its carbon emissions reduction targets over the past few years, including the goal of achieving zero CO_2 emissions by 2050 [2]. Like many other countries, Japan aims to achieve these goals in part by decarbonizing the energy sector, as well as electrifying sectors such as transportation as part of the Green Growth Strategy [3].

As of April 2022, the country's energy strategy towards 2030 is summarized in the 6th Strategic Energy Plan (6th SEP) [4]. Notably, the 6th SEP cites renewables as the top priority resource group, more than doubling solar PV and wind integration targets with respect to the 5th SEP, as well as introducing hydrogen/ammonia as a new resource to the planned energy mix for 2030 (Tab. 1).

Over the course of the 4th and 5th SEP, the foundation for integrating more variable renewable resources was laid through the introduction of an hour-ahead and renewable-friendly trading markets (which is to be continued more intensively over the timeframe of the 6th SEP), market access liberalization, as well as the vertical unbundling of transmission and distribution from generation [5, 6]. While the 6th SEP does not yet describe targets to move from more contract-focused to merit-order dispatch, the increased focus on (variable) renewables and market platform creation could suggest the emergence of a European-style system by 2030. The need for a system such as this, which is more flexible and competitive, has previously been discussed in the literature [7–11].

Japan aims for 20–30% of vehicles sold in 2030 to be battery-electric and around 3% fuel cell [12], with 100% of all vehicles produced in Japan by 2050 to be electrified [13]. With regards to specific drivetrains, the 2014 Strategic Roadmap for Hydrogen and Fuel Cells [14] aims for 800,000 fuel cell electric vehicles (FCEVs) by 2030. Additionally, 160 hydrogen refuelling stations (HRS) were planned for 2020, and 320 by 2025. These infrastructure developments are overseen by Japan H2 Mobility (JHyM), an organisation comprised of 11 companies [15]. For battery electric vehicles (BEVs), approximately 4.9 million BEVs are expected to be on the roads by 2030 [12, 16], with no specific targets for recharging infrastructure.

* Corresponding author: k.knuepfer@asagi.waseda.jp

Table 1. Comparison of 6th SEP with the previous 5th SEP target shares (%) by resource [4, 6].

Resource	Target share 5th SEP	Target share 6th SEP
Nuclear	20–22%	20–22%
LNG	27%	20%
Coal	26%	19%
Oil	3%	2%
Solar PV	7%	14–16%
Wind	1.7%	5%
Geothermal	1%	1.0–1.1%
Hydropower	8.8–9.2%	11%
Biomass	3.7–4.6%	5%
Hydrogen/Ammonia	—	1%

With this trend towards an electrified transport sector [17, 18], it becomes increasingly important to understand the hourly electricity demand curves of the various drivetrains and how they will impact the energy grid, in order to understand what would be the optimum maximum amount of renewables in the system and the optimal charging strategies [19, 20]. In this context, the CO_2 reduction potential of transport-integrated models has been extensively studied [21–25], together with the analysis of specific resource- and vehicle technology combinations [26, 27]. Studies have confirmed that electrified transport generally increases the penetration of intermittent renewable resources, [22, 24, 28–34], as well as helping to reduce the burden on the grid [34–39]. Specific drivetrains have also been found to support the integration of different resources more efficiently, with BEV electricity demand supporting solar PV integration particularly well [36, 37, 40–42], and FCEV electricity demand supporting wind more efficiently [21, 26, 35].

Refuelling/recharging infrastructure is an important demand-constraining factor, due to possible fuel/electricity supply bottlenecks. There may also be regional differences in these bottlenecks depending on charging/refuelling station density. Further, the various drivetrains require different infrastructure and supply chains. While BEV infrastructure connects relatively seamlessly to the electricity network, FCEV infrastructure requires separate conversion of electricity to hydrogen, and also transport and storage facilities (Lee *et al.*, 2014; [43]. In contrast to BEV infrastructure, the hydrogen supply chain for FCEVs can be decoupled from the electricity supply system if the fuel is sourced through, for instance, steam reforming [44]. While this is currently a common hydrogen-generating process, it will not be further considered in this study, as the Japanese Basic Hydrogen Strategy lays out plans to shift toward a system of hydrogen production from electricity from around 2030 to reduce its carbon footprint and revitalise regional economies [16].

The positive impact of electrified transport fleets on renewable energy integration and reducing grid burdens is often conditional on the assumption of grid-optimised charge scheduling, especially – though not exclusively – for BEVs [34, 42, 45–48]. Studies that have scheduled electrified fleets non-optimally find that the outcome is less efficient, but overall still beneficial to decarbonisation goals [34, 38, 46]. One likely reason why unscheduled charging is modelled less frequently is that it is difficult to get real vehicle use data with which to generate realistic demand patterns from driver profiles [39]. This is especially true for BEVs, though studies in the past have used internal combustion engine driving data to estimate FCEV profiles [34].

Driver profiles and user data (including distance covered and amount of time spent charging/refuelling, as well as number of times spent charging/refuelling per week/day and variations between days) are currently still rare [17]. For instance, Taljegard *et al.* [47] collected data on BEVs in the Västraland region of Sweden, from which they identified 200 unique driver profiles. Also at the regional level, Iacobucci *et al.* [49, 50] used transport survey data for Tokyo city. Richards (2013) also highlighted how models treat driver profiles computationally to estimate transport demand: as it is computationally expensive to recalculate the charge and driving status for each vehicle every hour, some studies have aggregated the vehicle fleet into one entity, so that there is effectively only one driver profile and one vehicle [51, 52]. Similarly, Tarroja *et al.* [34], aggregated a representative dataset of Californian vehicle travel data to represent the fleet of BEVs. As a result of this general lack of data and heavy reliance on assumptions, demand profiles for alternative fuel vehicles tend to be quite different between studies, even for the same region (see, for instance, the BEV profiles estimated for California by [34, 53, 54]. In Komiyama and Fujii's [30, 45] Japanese transport-integrated modelling study, the demand for electric vehicles is assumed to remain constant every day of the year and charging only takes place overnight (between 00:00 and 08:00) to minimise the computational cost. A different modelling approach has been pursued by Iacobucci *et al.* [49, 50], in looking at an autonomous, shared vehicle fleet in the Tokyo area. The role of a "profile" to make charging decisions is limited in this approach, as the vehicle can generally charge any time of the day in between trips. The authors model the battery charge levels of individual vehicles and regulate charging requests by, for instance, optimising for solar rooftop and wind generation availability [50]; or by requesting charging when an individual vehicle values electricity higher than its current price (the perceived value is inversely related to battery depletion levels) and by disconnecting from the charger at the price equilibrium point [49].

Among transport-integrated energy system modelling studies there is a focus on the regional (sub-grid) level [55–57], or the grid is ignored when trying to integrate transport demand [45]. While Taljegard *et al.* [47] do consider the grid and transport demand, their study only consists of two regions. Further, studies either assess the impact of integrating one-vehicle technology [41, 42, 45, 47, 49, 50, 58] or the comparative performance of different technologies on specific outcomes [28, 34], while few studies model more than one technology in the system concurrently [55, 56]. Despite the lack of concurrent transport-integrated energy system modelling studies, the value of mixed-fleet studies in identifying synergistic technology mixes [27, 34, 38, 59], as well as challenges due to interactions between components [21] has been recognised.

Based on these gaps, this study has two objectives. First, to estimate the transport demand curves for BEVs and FCEVs in Japan, based on the 2030 target fleet size and infrastructure. Second, to estimate the impact on the energy mix that will result when multi-drivetrain transport demand is integrated into a country-level energy system with a transmission grid. The overall contribution of the paper resides in the integration of a system that can accurately reproduce the electricity production of intermittent sources, with both a transmission grid that can meet the demands of energy of the different regions of Japan and also of BEVs and FCEVs. While some simplifications exist at different levels within he model, the authors hope that EnSym will eventually be able to provide policymakers with an easy-to-use tool that can help see the outcomes of different strategies and policies.

2 Methodology

2.1 Model overview

EnSym was programmed in VBA by the authors, with the data being compiled in Python 3 and stored in an SQL database (see Knuepfer *et al.* [8]). The model simulates both traditional and transport-based hourly electricity demand, as well as all major electricity supply and storage sources. It can also adopt different dispatch hierarchies and take into account inter-regional electricity transmission limitations in the target country. The model so far has only been applied to the case of Japan, although it should be noted that it simulates the sub-division of regions and major metropolitan areas (MMAs). All prefectures in Japan are included in the model except Okinawa, an island archipelago to the south of the country that is not connected to the main grid.

Once the dispatch hierarchy, the installed capacity of each resource in each region and the target share of each resource in the energy mix have been set, the main model workflow basically consists of three steps. First, the hourly potential generation capacity and electricity demand for each region are estimated. Second, based on these estimates, each region sets its own hourly resource generation targets to meet the annual desired target share set by the user of the software. Third, electricity is traded between the regions to fulfil electricity supply targets and avoid blackouts via the transmission grid. Grid trading and balancing are conducted taking into account spatial proximity between demand and supply as well as the direction of flow, with the model not allowing for looping of transmission volumes. For further details on EnSym, see Knuepfer *et al.* [8].

In this study, the authors expanded the EnSym model to include electrified transport sector electricity demand, which was estimated using Python 3 and C++. EnSym thus improves on previous combined transport and energy system models which did not include transmission grid constraints (*e.g.* [45, 55–57]. While Taljegard *et al.* [47] do include both, these authors only consider one type of drivetrain (BEVs) and their system is subdivided into only two regions. Table 2 highlights the operational parameters on which EnSym improves on from those in the existing literature.

2.2 Electricity supply

2.2.1 Installed capacity targets

On the supply side, all major electricity-generating and storing resources relevant to the year 2030 are simulated, including utility-scale batteries and pumped hydro storage. The Ministry of Economy, Trade and Industry (METI) has outlined a target of installed generation capacities for 2030 for most resources at the country level [60]. This includes 88 GW solar PV, 1.4–1.6 GW geothermal, 13.3–15.3 GW wind, 7.2 GW of biomass, and focused growth of small- to mid-scale conventional hydropower plants from 9.7 GW to 10.94–11.65 GW. The installed capacity of thermal power will be reduced while maintaining an "appropriate thermal portfolio" [60]. Given the unchanged generation share target for nuclear power between the 5th and 6th SEPs, the authors assume that the target capacity for this resource will remain at 38 GW [61]. Where ranges were published, the authors chose the mean value.

Among the planned resource capacities, the authors chose to slightly alter the installed capacity of nuclear power and solar PV. Of the planned 38 GW nuclear power, only 33.2 GW are likely going to still be operational, with no additional new plants having made enough progress to expect them to be operational by 2030 (see the Appendix). The planned 88 GW of solar PV capacity by 2030 seem to be an underestimation, based on the most recent information on installed and approved solar PV capacities under the FiT scheme, which is 139.12 GW [62]. Therefore, the authors amended the target solar PV capacity to 139.12 GW for 2030. The wind resource includes both on- and offshore capacity, in line with the government target of 10 GW [60]. As no capacity targets for LNG, coal and oil were published as of April 2022, these resource capacities were assumed to remain unchanged from the 2021 estimate (see Knuepfer *et al.* [8]), which is a conservative estimate, given the planned reduction in their generation target shares.

The regional pattern of the distribution of resource capacities remains mostly unchanged from Knuepfer *et al.* [8] and, in the case of offshore wind, Chen *et al.* [63]. Any increase or decrease in capacity at the national level was distributed proportionally amongst regions based on this (see Appendix for regional changes). Table 3 summarises the resource distribution by region as projected for 2030.

Further, utility-scale batteries were also expected to be installed [64], with the capacity assumed to remain unchanged between 2020 and 2030, based on the lack of more detailed information available (Table 4).

Table 2. Research gaps in existing models to be addressed through EnSym.

Model by author	Point of improvement
Zhang *et al.* [57]	Only regional (Tokyo area), does not account for the electricity grid.
Felgenhauer *et al.* [55, 56]	Only regional (Freiburg (Germany) and Palo Alto (California), do not take into account the electricity grid.
Komiyama and Fujii [45]	Only integrate one vehicle technology, not considering the electricity transmission grid to reduce computational complexity.
Taljegard *et al.* [47]	Only integrate one vehicle technology, and their grid consists of only two regions (Scandinavia and Germany).

Table 3. Expected installed capacity (GW) of each resource in each region of Japan in 2030.

Resource	METI projection	Japan total	Hokkaido	Tohoku	Kanto	Chubu	Hokuriku	Kansai	Shikoku	Chugoku	Kyushu
Coal	51.9	51.9	1.9	4.3	17.3	7.5	0.8	9.6	1.9	3.3	5.3
LNG	84.9	84.9	3.1	7	28.2	12.3	1.4	15.7	3.1	5.4	8.7
Oil	30.8	30.8	1.1	2.5	10.2	4.5	0.5	5.7	1.1	2	3.1
Nuclear	38	33.2	2.1	2.8	1.1	3.6	11.3	6.5	0.9	0.8	4.1
Hydro Conventional	23.75	23.75	1.4	3.9	1.5	8	4	0.87	0.98	1.1	2
Hydro pumped	27.47	27.47	1	0.5	5.3	10.1	1.6	4	0.6	2.1	2.3
Solar PV	87.6	139.12	4.27	16.06	52.37	15.15	1.2	12.2	3.66	7.8	26.4
Onshore wind	14.3	14.3	2.2	5.2	0.46	0.7	0.47	1.39	0.7	1.28	1.86
Offshore wind	10	10	1.5	4.5	0.4	0	0.7	0.7	0	0	2.2
Geothermal	1.5	1.5	0.08692	0.85	0.00005	0.00057	0.00024	0.00010	0	0.00005	0.55483
Biomass	7.2	7.2	0.32	1.14	1.08	1.26	0.58	0.6	0.42	0.92	0.9
Total	367.42	414.14	17.47	44.25	117.5	63.11	21.8	56.56	13.36	24.7	55.21

2.2.2 Electricity generation potential

EnSym estimates potential electricity generation for each resource on an hourly basis throughout an entire year. The hourly electricity generation potential for solar PV and wind was calculated using meteorological data from one meteorological station per prefecture [65]; see Appendix for a list of the stations used). For thermal resources, the authors assume that no maintenance is required throughout the year -no fluctuation in the generation potential- and that the generation potential depends only on the capacity factor. Both pumped hydro and utility-scale batteries are determined to be driven by variable renewables, that is, wind and solar PV (which allows the authors to categorise these two types of storage as renewable). All pumped hydro stations and utility-scale batteries are assumed to have the same capacity throughout the country (see Knuepfer *et al.* [8].

2.3 Traditional electricity demand

EnSym considers both hourly traditional as well as transportation electricity demand from BEVs and FCEVs. The total annual traditional electricity demand for 2030 was estimated at 1065 TWh [3]. The hourly traditional demand curve for each prefecture was estimated by the authors using the following procedure: First, the annual expected electricity demand for 2030 [3] was distributed over each prefecture and month based on monthly electricity demand estimates from 2017 [66]. The resulting monthly electricity demand estimates for 2030 by prefecture were distributed over each hour of the month by using the hourly demand data for the Kanto region [67] as a representative weighting factor (see Knuepfer *et al.* [8].

2.4 Transport electricity demand

2.4.1 BEV charging infrastructure

BEV charging infrastructure is divided into private and public chargers. As official data [68] only provides information as to the number of chargers available in each prefecture and whether they are slow- or fast-charging, all public charging stations were assumed to have two dispensers (*i.e.* two cars can charge simultaneously). Private chargers were assumed to make up 10.6% of all chargers [69] and to be exclusively installed in single-family homes, with one charger per home and per car (among those that have private chargers).

The total BEV charging infrastructure distribution in 2018 [68] is also assumed to be representative of 2030. To distribute the chargers between each MMA and the rest of each region, the distribution of the human population in and outside of an MMA [70] was used as a ratio. While

Table 4. Announced, commissioned and operational large-scale battery-rated power (MWh) as of 2021 (Source: [64]).

Storage medium	Japan	Hokkaido	Tohoku	Kanto	Chubu	Hokuriku	Kansai	Shikoku	Chugoku	Kyushu
Battery	910	73.8	323.5	180.8	0.0	0.0	2.7	0.0	25.3	303.9

Table 5. Number of public and private BEV chargers by region and MMA within a region estimated for 2030.

Region	Public chargers		Private chargers	MMA	Public chargers		Private chargers
	Normal	Fast			Normal	Fast	
Hokkaido	1365	661	278	Sapporo	495	239	46
Tohoku	3398	1720	465	Sendai	451	113	43
Kanto	20888	3694	2227	Tokyo	8990	1161	918
Chubu	10600	2127	955	Shizuoka-Hamamatsu	755	72	47
				Chukyo	2015	260	93
Hokuriku	1614	822	155	Niigata	218	46	28
Kansai	8616	1791	1167	Keihanshin[1]	2250	509	258
Chugoku	2918	1134	385	Okayama	786	186	28
				Hiroshima	447	165	40
Shikoku	1082	1162	199	–	–	–	–
Kyushu	4417	1641	674	Kitakyushu-Fukuoka	910	94	99
Japan total	54898	14752	6505	Of which in MMAs	17317	2845	1600

[1] The Keihanshin MMA includes Kyoto, Osaka and Kobe cities.

the share of private chargers per region is assumed to be fixed at 10.6%, it is also assumed to be unequally distributed between MMAs and the rest of each region, as most private chargers as of 2016 are estimated to be installed in detached houses, which are more often situated outside of the MMAs [69, 71].

It is further assumed that chargers are not capable of bi-directional flow; that is, electricity generation from vehicle to grid is not possible (V2G). The final distribution of the approximately 76,155 BEV chargers expected by 2030 is summarized in Table 5.

2.4.2 FCEV refuelling infrastructure

The number of Hydrogen Refuelling Stations (HRSs) per city is provided by CEV [72]. While a minimum of 320 HRS is expected to exist by 2030 in Japan [16], this work uses only the 135 HRS available in June 2020 (see Tab. 6).

The authors decided to not increase the number of HRS in 2030 based on 3 assumptions. First, in contrast with BEV chargers, the current HRS distribution is less likely to be geographically representative of the 2030 distribution due to a different expansion strategy [73]. Second, in contrast to BEV chargers, the number of dispensers per HRS can vary more. While the currently installed HRS can be assumed to have only one dispenser each (based on their hourly dispensing volume), the number of dispensers per site will likely increase as the fleet size grows, which further decreases the representativeness of the current HRS infrastructure for extrapolation to 2030. Lastly, the authors argue that the simulation can run smoothly with the current number of HRS and fleet size, as the current ratio of vehicles per HRS would be 5926 which – while above the current ratio of combustion engine vehicles to petrol stations in Japan (roughly 2033 vehicles per station [74]) – is still likely within the norm of a developed country in general (*e.g.* Germany's ca. 4558 vehicles per station [75]).

HRS infrastructure is exclusively public, with only the hourly dispensing volume known, but not the number of dispensers per HRS. To estimate the latter, the authors used the HRS standardization chart defined by H_2 MOBILITY Germany (see Table 7).

It is assumed that each HRS provides H_2 at each FCEV's optimal pressure (350 or 700 bar) in all cases and that it is exclusively generated through electrolysis using an Alkaline Electrolyser (Table 8).

2.4.3 The vehicle fleet

The entire fleet of alternative fuel vehicles (AFVs) is assumed to be comprised of two BEV models (Nissan Leaf II and Tesla Model 3) and one FCEV model (Toyota Mirai). The modelling of the drivetrain specifications is described in the Appendix).

The AFV fleet was distributed between MMAs and the rest of each region according to the distribution of the private chargers and the ratio between public chargers in metropolitan areas and the countryside [68]. The relation between infrastructure availability and AFV distribution in turn influences refuelling/charging decisions and therefore transport demand curves in each region. The total number of BEVs and FCEVs as of 2018 and that expected by 2030 is summarized in Table 9 (note that this does not include diesel and various hybrid vehicles).

Table 6. Number of HRS by region and size in 2020 (Source: [83]).

Region	Very small	small	MMA	Very small	small
Hokkaido	2	0	Sapporo	2	0
Tohoku	2	2	Sendai	0	1
Kanto	17	35	Tokyo	15	30
Chubu	15	22	Shizuoka-Hamamatsu	1	2
			Chukyo	14	20
Hokuriku	1	0	Niigata	1	0
Kansai	4	14	Keihanshin	2	12
Shikoku	3	0	–	–	–
Chugoku	4	1	Okayama	1	0
			Hiroshima	3	0
Kyushu	4	9	Kitakyushu-Fukuoka	2	8
Japan total	52	83	Of which in MMAs	41	73

Table 7. HRS size standardization according to H2 Mobility Germany (IEA [84]).

Parameter	Very small	Small	Medium	Large
Number of dispensers	1	1	2	4
Refuellings/hour/dispenser	2.5	6	6	10
Maximum number of refuellings/day	20	38	75	180
Maximum hourly H_2 output (kg)	18	34	67	224
Maximum daily H_2 output (kg)	80	212	420	1000

Table 8. H_2 electrolysis technology [85].

Parameter	Unit	Value
Technology type	–	Alkaline Electrolyser
Stack unit size	MW	1
Electrical efficiency (stack)	kWh/kg H_2	47–66 (49 in this work)
Lifetime (stack)	Hours	60,000

Table 9. Passenger vehicle diffusion in Japan in 2018 and 2030 projections (Source: [12, 16]).

Technology	2018	2030
Total passenger vehicles	61,558,464	61,590,000
Internal combustion engine	51,887,281	18,477,000–30,795,000
BEV	112,242	4,927,200
FCEV	3,009	$\leq$800,000

The number and distribution of AFVs by region and MMA is estimated based on information on such vehicles purchased with subsidies [12, 68] and it is assumed that the concentration of refuelling/recharging infrastructure is related to vehicle purchase decisions in each region and MMA. For details regarding the estimation, please see the Appendix. The resulting number of BEVs and FCEVs is provided in Table 10.

Assumptions regarding the characteristics of the vehicle fleet include that:

- BEV (dis-)charge behaviour is constant, irrespective of the charge level (that is, the battery does not (dis-)charge faster or slower when it is already relatively full or empty, which is a conservative estimate);
- There is no battery degradation in the fleet;
- There are only two BEV and one FCEV vehicle technologies on the market (which also means that the assumptions about their efficiency will be outdated (and hence conservative) in a decade;
- No other mode of transport places further electricity demands on the grid (such as non-passenger vehicles or hybrid cars);
- All drivers behave in accordance with the average energy consumption per 100 km of their respective vehicle.

2.4.4 Driver profiles

To estimate the transport demand curve, as a first step some characteristics of vehicle drivers were considered (driving distance, timing, and charging/refuelling needs).

Table 10. Projected number of vehicles by region within the MMAs and by technology by 2030 (Source: [12]).

Region	BEV	FCEV	MMA	BEV	FCEV
Hokkaido	72,079	3,445	Sapporo	26,213	1,722
Tohoku	370,170	25,100	Sendai	36,715	5,167
Kanto	1,512,636	364,442	Tokyo	709,586	178,653
Chubu	926,887	283,974	Shizuoka-Hamamatsu	89,653	6,767
			Chukyo	176,634	861
Hokuriku	162,011	1,230	Niigata	24,758	135,835
Kansai	814,120	69,886	Keihanshin	226,478	27,068
Shikoku	291,062	11,566	–	–	–
Chugoku	104,908	10,089	Okayama	54,627	1,353
			Hiroshima	46,937	1,476
Kyushu	646,127	30,268	Kitakyushu-Fukuoka	151,408	11,934
Japan total	4,900,000	800,000	MMA total	1,543,009	370,836

The rules according to which drivers decide whether, when and how far to travel, as well as basic decision-making during the refuelling/charging process, are defined as the "driver profile". Each parameter in the driver profile is constrained by boundary values and sub-divided into weighted range groups based on assumptions by the authors or previously observed patterns for each drivetrain (for details, please see the Appendix). Each vehicle is randomly assigned into one of the weighted range groups (based on [69], and within the assigned range group they are again randomly assigned a daily driving distance value. To further reduce the level of synchronicity between the vehicles in the fleet, every vehicle is randomly assigned an initial tank/battery fill level at the beginning of the simulation.

Two driver profile patterns were defined for each technology, namely "commuter" and "leisure". The commuter profile is relatively well established in terms of driver behaviour, with assumptions regarding commuting periods being based on Zhang *et al.* (2020), and the interval between commutes being approximated from the day-time BEV charging duration given in Pareschi *et al.* [76].

For the case of the leisure profile Taljegard *et al.* [47] observed that driver behaviour throughout the day is relatively random: to represent the demand pattern observed from 429 GPS-tracked petrol cars, Taljegard *et al.* [47] extracted 200 unique driver profiles. Based on this, it can be assumed, that the 24 leisure profiles generated in the current study are unlikely to be fully representative (just as the commuter profile does not realistically cover the full bandwidth of actual commuter driving patterns). However, both profiles can be useful to broadly represent distinctly different types of drivers using a relatively computationally efficient method to do so and thus diversify the fleet.

2.4.5 Infrastructure use rules

As alternative fuel vehicles move through the day and use fuel (either electricity or electrolysed hydrogen), they eventually will request to connect with a charger or HRS. Apart from driving and resting-related rules, this simulation also sets five basic rules that govern the use of infrastructure and its constraints (for detailed definitions of the parameters, see the Appendix):

- First, the rules for refuelling/ charging describe the general process and duration of the connection.
- Second, infrastructure preference describes the rules by which types of chargers (home, public) or HRS will be preferred by a driver.
- Third, the queueing rule describes the decision-making procedure that vehicles undergo when their request to connect to refuelling/charging infrastructure is unsuccessful. The outcome of this procedure is that only those that most urgently need it will queue for charging/refuelling, so that the simulation completely avoids empty tanks/batteries (as at a specified depth of discharge drivers refuse to move further), and that it generates more variability in movement patterns, as drivers can forego or delay their planned activities to queue.
- Fourth, the reconnection intervals rule defines how long a vehicle needs to wait after disconnecting from refuelling/charging infrastructure before it can reconnect again. The purpose of this is to ensure that, in case of infrastructure bottlenecks, all vehicles wanting to connect get a similar chance to do so.
- Lastly, the movement delay rule defines how vehicles adapt their movement schedule (consisting of driving, parking and home hours) if an activity overlaps with queueing (which takes priority).

2.5 Transmission

EnSym assumes regional electricity transmission constraints for the year 2030 that are based on the grid connections that are outlined in OCCTO [61]. Additionally, a fixed 5% heat loss is assumed for each hourly transmission volume. Figure 1 provides an overview of the transmission constraints by region (See Knuepfer *et al.* [8]).

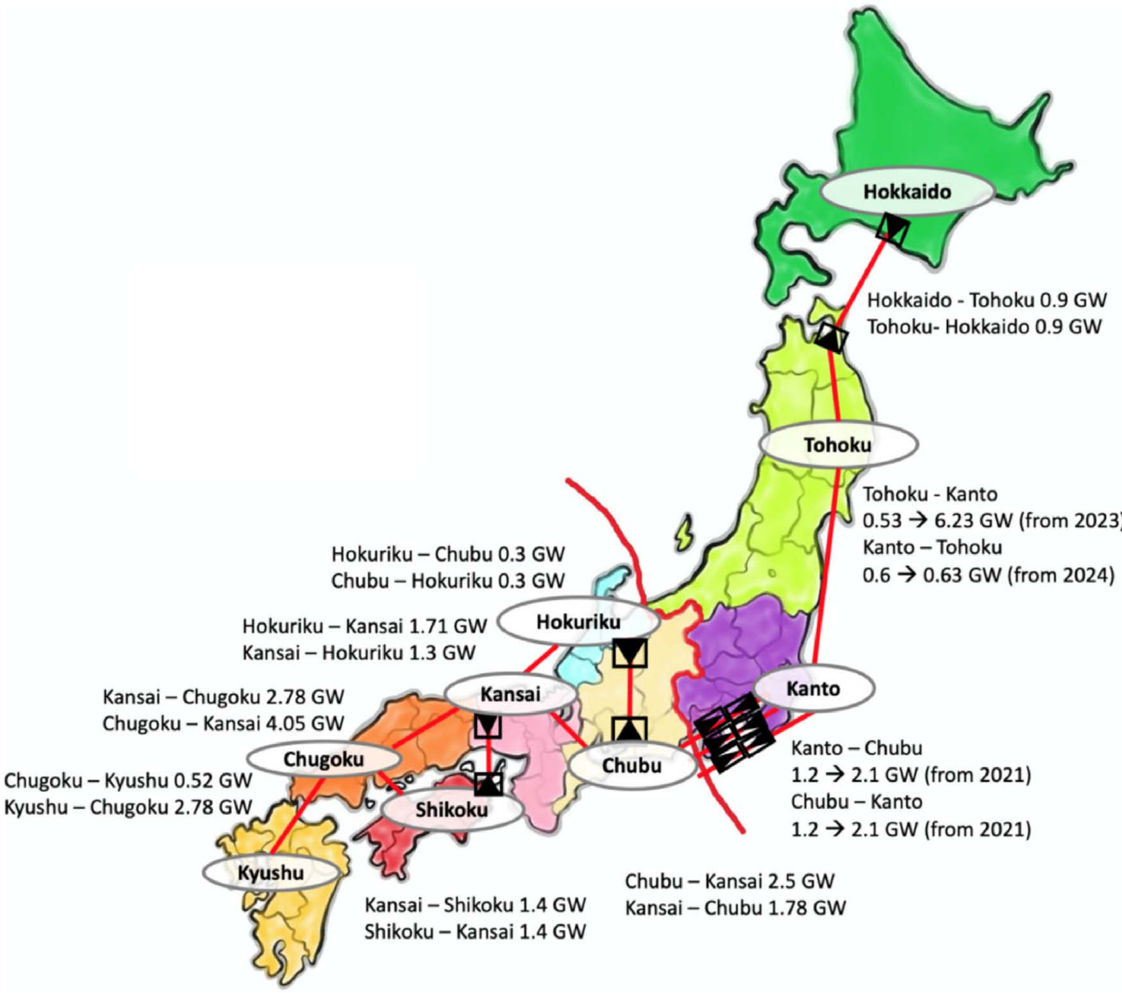

Figure 1. Capacity of each major transmission line in the grid, with DC lines marked by triangles and AC lines without (Source: OCCTO, 2019). The dates inside the brackets indicate when the increased capacity should be available.

2.6 Scenario setup

To meet the first objective of this study, the authors generated the annual electricity demand curves for each vehicle drivetrain. To meet the second objective of this study, a business-as-usual (BAU) base case for the 2030 energy mix was simulated without electricity demand from transport and assuming a merit order dispatch of renewable resources, given the focus of prioritizing and maximizing renewable generation stated in the 6th SEP. Further, a *transport-integrated scenario* was defined to estimate the change in the energy mix resulting from the integration of transport demand.

The total estimated electricity demand for 2030 according to METI [3] is 1065 TWh, including transport-derived electricity demand. To estimate the expected electricity demand for the BAU (which does not include electricity demand for transport), the transport demand share therefore needs to be deducted. To do so, the authors assumed that the transport demand estimated through the present model (based on the 2030 fleet and infrastructure) is going to be representative of the 2030 transport electricity demand, and simply deducted it from the overall consumption for the case of the BAU.

The scenario setup is summarised in Table 11.

3 Results

3.1 Transport demand estimation

3.1.1 Vehicle fleet characteristics

The two driver profile patterns defined in the methods section ("commuter" and "leisure") were applied to both FCEVs and BEVs. The model determined the number of unique subsets possible for each technology taking into account the movement plan based on the flexibility of driving hours, which gave a number of possible unique profiles of $N = 24$ for each driver type and $N = 48$ for each technology. This number was used for the FCEV fleet, though for the BEV fleet, an additional movement plan was generated for each subset, resulting in $N = 50$. This additional movement plan for each subset is a duplicate in terms of its

Table 11. Scenario setup in EnSym.

Scenario	Installed capacity	RES-E generation share (%)	Dispatch strategy	Demand (TWh)
BAU	6th SEP; Knuepfer *et al.* [8]	6th SEP	Merit	1065 – (model-derived transport demand)
Transport-integrated	6th SEP; Knuepfer *et al.* [8]	Estimated through the simulation	Merit	1065

planned movement schedule. However, the assigned daily driving distance and battery charge state at the beginning of the simulation are still unique to each individual driver. The additional movement plans were added to illustrate how the movement plans of the BEV fleet should be more diversified than that of the FCEV fleet (which would be otherwise identical). This can be observed when comparing the BEV (Fig. 2b) and FCEV leisure driver movement plans (Fig. 3b).

Figures 2 and 3 provide an overview of the number of subsets for each driver profile and technology, which plan to move at a given hour of the day. Note that the number of subsets in Figures 2 and 3 adds to twice the number of subsets for each driver type, as each subset should drive twice a day.

For the BEV fleet (*i.e.* both commuters and leisure drivers) it can be observed that all vehicles are expected to park between 11:00 and 13:00 on weekdays, (and in the case of leisure drivers, also weekend) and that the entire BEV fleet (all four subset groups) is also expected to be at home between 22:00 and 05:00 h. This generally agrees with the localised charging peak around midday for BEVs that was observed by Pareschi *et al.* [76]. For the BEV fleet, most of the morning charging should arise from the leisure fleet, and the midday charging from the commuter fleet. Alterations are possible, as vehicles can shift their movement plans during the simulation based on the movement delay parameter (as described in the methodology). For FCEVs, the planned movement curves are similar, though less nuanced, due to the lesser number of driver profiles ($N = 48$ instead of 50). Refuelling timing is not as predictable as in the BEV fleet, due to shorter connection times with a HRS.

Apart from driving times, the second component of diversifying fleet behaviour is the randomisation of the other parameters shown in Tables A8 and A9 in the Appendix, such as for example the daily driving distances for each technology, see Figure 4. The line in each box shows the median daily driving distance for each vehicle model group and the "X" is the mean daily driving distance. Half of all observations fall within the boxes, with individual points outside showing outliers. It can be seen that 75% of all commuters drove less than 70 km/day, with a mean distance of 40–60 km/day. The leisure subsets saw greater variation in their 50% range, with the Nissan Leaf drivers highly concentrated in the 20–40 km/day range, while Tesla drivers had the most spread-out driving distances at 20 to around 100 km/day. This difference between technologies is also influenced by the specific maximum ranges.

3.1.2 Estimating transport demand

The 2030 mixed technology fleet would be comprised of 4.9 million BEVs and 800,000 FCEVs, which would account for an estimated annual electricity demand of 55 TWh and 0.51 TWh respectively, which would mean that transport would comprise 5.21% of the total estimated electricity demand by that date (See Table 12).

The hourly demand curves for each vehicle technology would present no seasonal variations and are assumed to be repetitive on a weekly basis. Regional differences are based on the number of cars, as well as the density of charging/refuelling stations (see Fig. 5 for BEVs and Fig. 6 for FCEVs).

FCEV demand peaks in the early morning (around 8:00 h), followed by a sharp drop as drivers begin their daily activities. It picks up again at the beginning of the afternoon, but is overall relatively flat throughout the day, with less pronounced diurnal variation than the BEV demand curves. This is partially due to the shorter refuelling duration, and partially due to the lower-than-expected HRS:FCEV ratio (the number of HRS was not increased between 2020 and 2030, as discussed in the methodology section). Hence, available dispensers are constantly occupied, even during the night. Lastly, the FCEV demand curve is also shaped by the fact that H_2 is assumed to be electrolysed on-site at the HRS, rather than being stored and distributed from centralized storage facilities or pipelines, which would result in a much more variable demand curve than the one observed in Figure 7.

BEV charging on the other hand requires at least one - usually several- hours of parking. The flat demand overnight (Fig. 8) indicates that the number of drivers connecting during the night is steady (*i.e.* mainly – but not exclusively – due to those owning home chargers, who have guaranteed access). Further, as most of the BEV fleet is scheduled to be parked between 11:00 and 13:00 h on weekdays, this leads to a sustained midday peak in demand. The regional differences in electricity demand on weekdays and weekends derive in part from chance (as driver profile parameters are randomly generated), and in part from how urbanized the region is (*i.e.* a difference in the number of detached houses, home chargers, and vehicle density compared to the number of chargers).

3.2 The BAU energy mix

Deducting the transport-derived electricity demand stimated in the previous section (55.81 TWh) for each hour

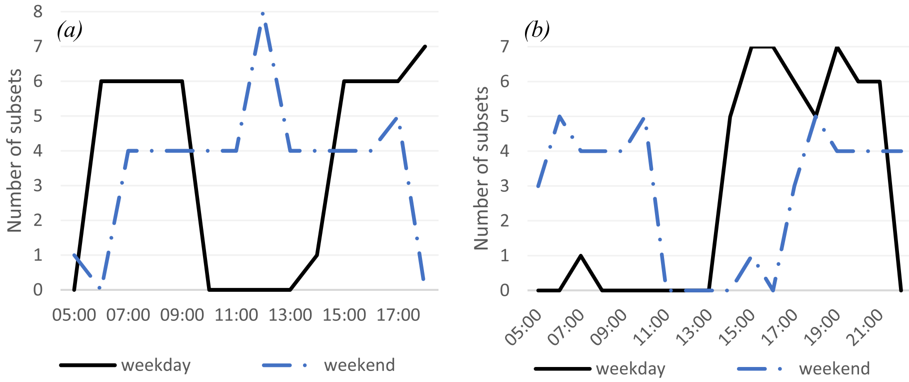

Figure 2. Combined planned movement of BEV commuter (a) and leisure (b) subsets throughout the day.

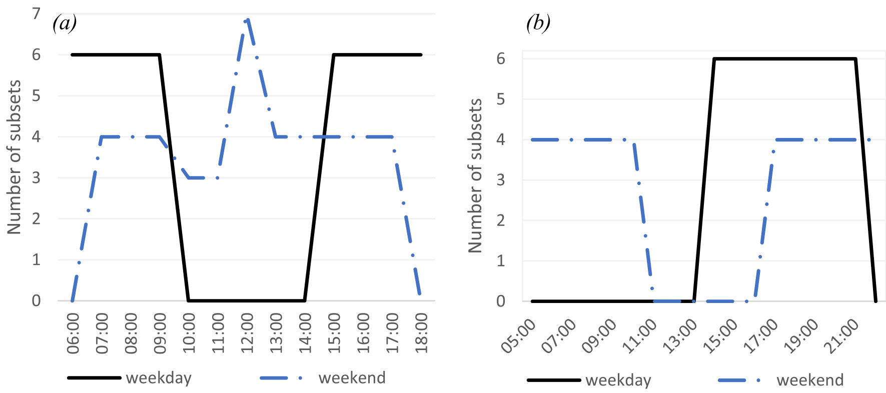

Figure 3. Combined planned movement of FCEV commuter (a) and leisure (b) subsets throughout the day.

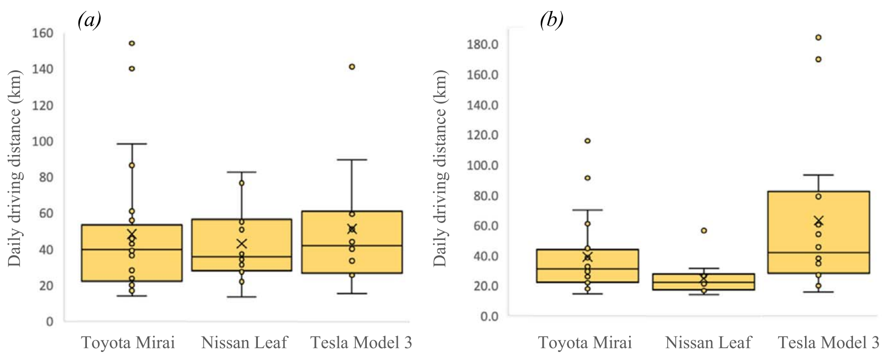

Figure 4. Distribution of daily driving distance by car model for the commuter (a) and leisure(b) subset.

from the total estimated electricity demand for 2030 (1065 TWh), the total BAU electricity demand was determined at 1009.19 TWh. Figure 9 shows the estimated BAU energy mix without transport demand, which indicates that several resources are likely to fall short of the 6th SEP target shares set for 2030 (see Fig. 9). For instance, solar PV only reached a 10.2% share (target: 14–16%), biomass 4.2% (target: 5%), wind 2.8% (target: 5%), geothermal 0.9% (target: 1%) and hydro 8% (target: 11%). These deficits were balanced by increased generation shares from oil (2.8% instead of 2%) and particularly LNG (30.5% instead of 20%).

The energy mix varies each hour and day, particularly given the availability of variable renewable resources. For instance, despite the 9th of August being one of the days of the year with the highest electricity demands in Japan, PV production exceeds the planned 14–16% (see Fig. 10 and Table 13).

3.3 The transport-integrated energy mix

For this scenario, total demand was estimated at 1065 TWh, *i.e.* including 55.81 TWh of transport demand. The resulting energy mix is summarized in Figure 11.

Table 12. Annual transport demand and number of vehicles by region and technology for 2030.

Region	BEV (GWh)	FCEV (GWh)	BEV (number of cars)	FCEV (number of cars)
Hokkaido	1,184	4	72,078	3,445
Tohoku	4,700	34	370,169	25,100
Kanto	15,590	248	1,512,635	364,442
Chubu	10,570	94	926,886	283,974
Hokuriku	3,267	23	162,011	1,230
Kansai	7,340	48	814,119	69,886
Shikoku	2,422	23	291,062	11,566
Chugoku	2,812	26	104,908	10,089
Kyushu	7,417	10	646,126	30,268
Japan	55,303	510	4,900,000	800,000

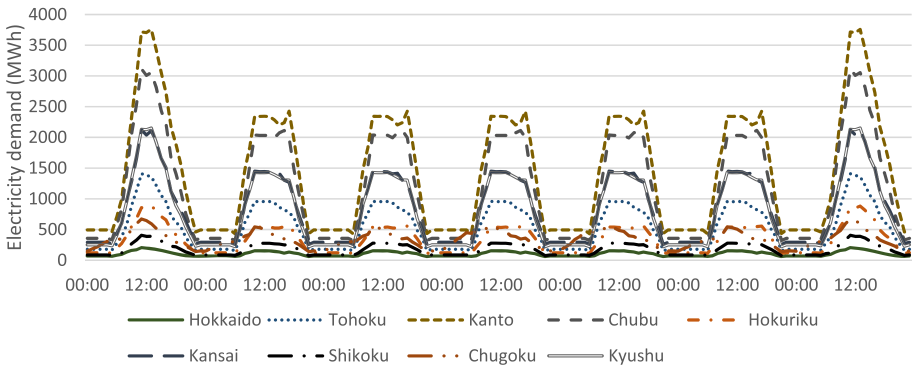

Figure 5. Weekly demand due to BEV region (2nd–8th January).

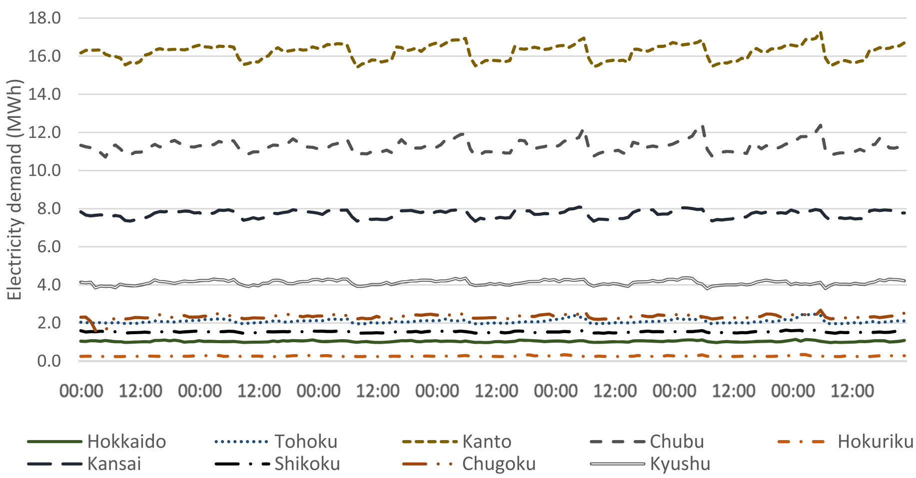

Figure 6. Weekly demand due to FCEV region (2nd–8th January).

It can be seen that while the generation shares of coal, batteries, geothermal and solar PV remained basically the same or increased slightly, the shares of all other resources decreased, except for oil, which increased from 2.8% to 4% for 2030. The reduction in generation shares for most resources is partially due to the changes in demand between regions due to the introduction of transport demand. In regions where demand has increased significantly, resource capacities would need to be increased to maintain their generation shares with respect to the BAU. For instance, the energy mix on the 9th of August shows that while the shares of biomass, geothermal, solar PV, wind and LNG decreased, their overall generation volume increased with respect to the BAU scenario (see Fig. 12 and Table 14).

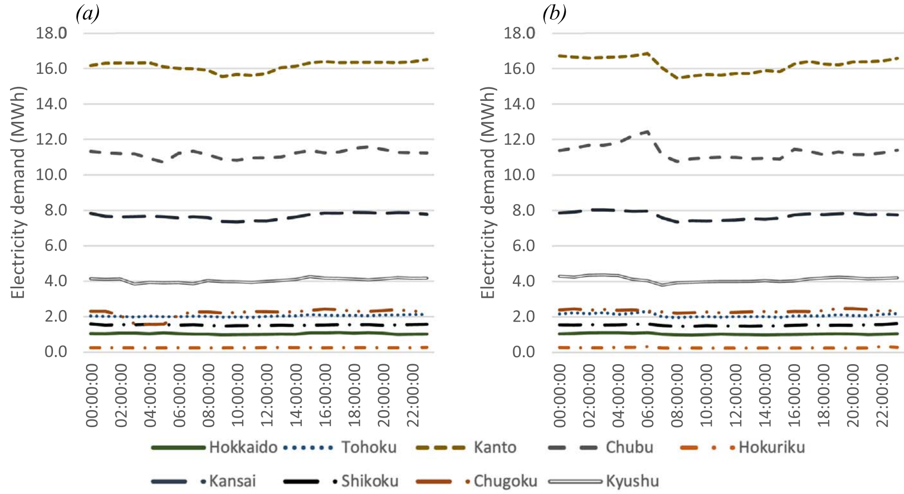

Figure 7. Weekday (a) and weekend (b) FCEV demand for electrolysis directly at the station.

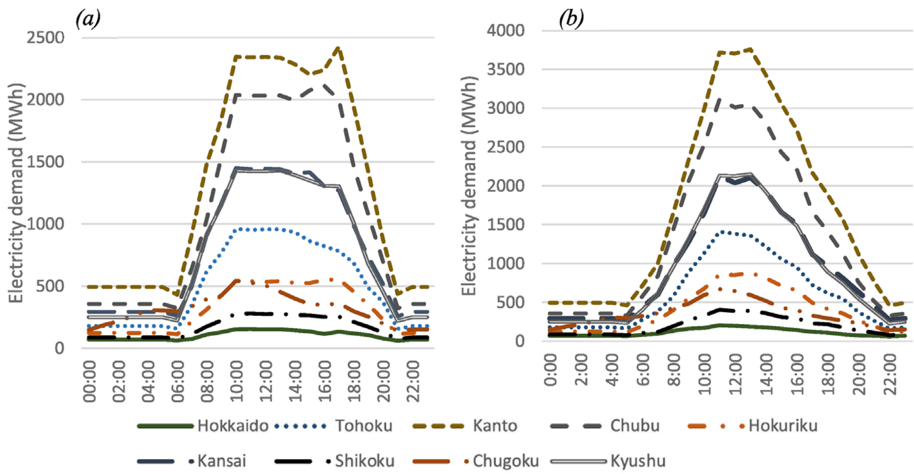

Figure 8. BEV demand on Tuesday, 3rd (a) and Sunday, 8th (b) of January.

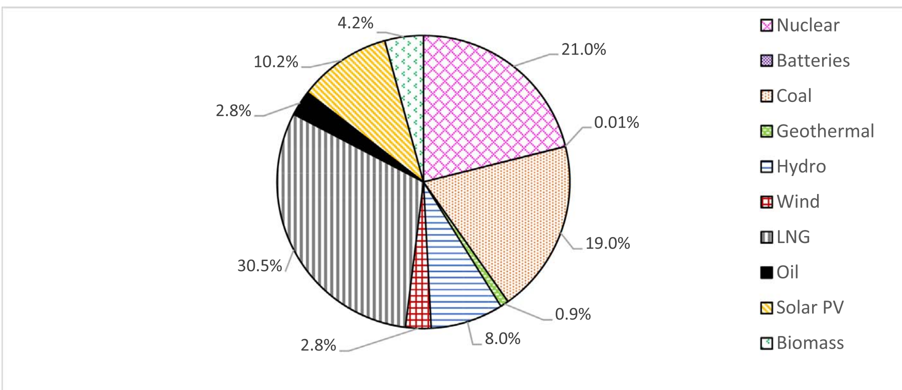

Figure 9. The BAU energy mix (%) for 2030 without transport demand.

Regions with a relatively larger increase in demand in the transport-integrated scenario also have a relatively larger installed capacity of oil (Kanto and Kansai alone have over half of the installed oil generation capacity of Japan as of 2022). This suggests that the increase in oil generation was likely due to local requirements in only a couple

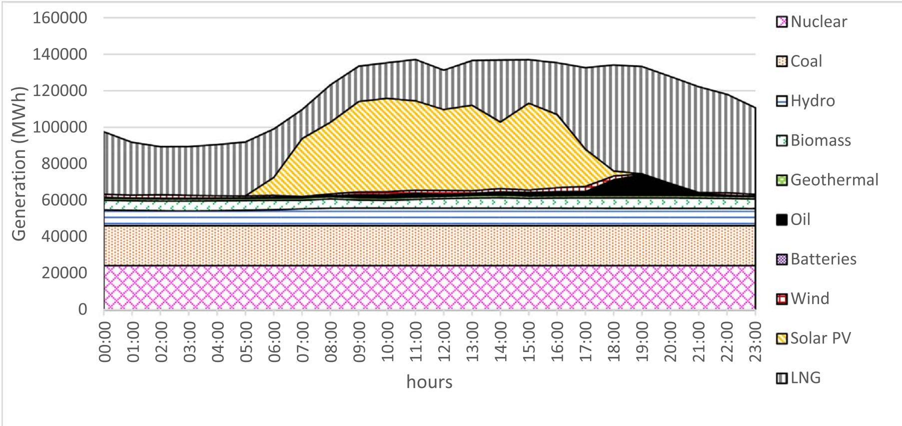

Figure 10. Hourly generation by resource (MWh) on the 9th of August.

Table 13. Total generation by resource (GWh) on the 9th of August.

Resource	Nuclear	Coal	Hydro	Biomass	Geothermal	Oil	Batteries	Wind	Solar PV	LNG
GWh	580.6	525.3	220.8	127.3	30.4	47.0	0.3	33.8	469.0	810.1
%	20.41	18.47	7.76	4.48	1.07	1.65	0.01	1.19	16.49	28.48

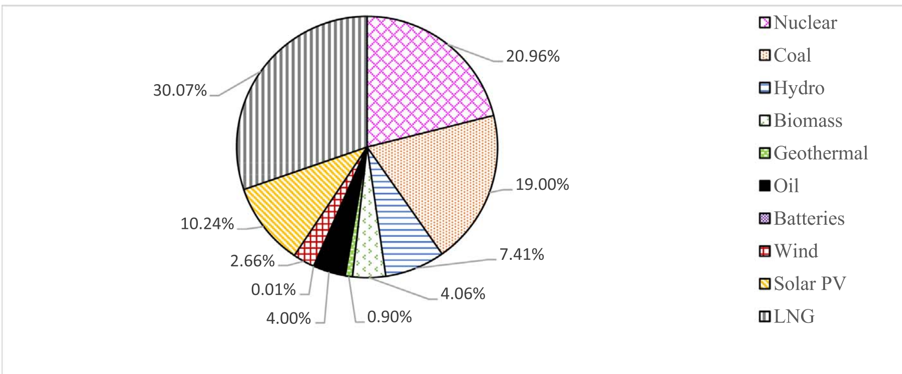

Figure 11. The energy mix (%) for 2030 including transport demand.

of regions (most demand increase comes from the Kanto and Kansai vehicle fleets), which could not be met by more renewable resources due to insufficient local capacity and constraints in the transmission grid. This is also likely the reason why LNG generates an approximately 10% larger share in the annual energy mix than planned for in the 6th SEP.

3.4 Comparative global warming potential

As the target of the Japanese energy strategy is to have zero CO_2 emissions by 2050 (Nikkei, 2020), it is relevant to understand the global warming potential of the energy mix. Table 15 shows the global warming potential for utility-scale batteries [77], offshore wind [78] and all other major resources [79].

Table 16 provides an overview of the annual generation volume and share, as well as the global warming potential of each resource. While the total generation volume increased by 5.3% between the BAU and the transport-integrated scenario, emissions increased by 3.7%. The largest sources of emissions were coal (44.64% and 45.41% of total emissions for each scenario, respectively), LNG (37.73% and 37.78% of emissions respectively) and conventional hydropower (15.09% and 14.23% of emissions respectively). Of the total emissions increase from the BAU to the transport-integrated scenario, 96.4% were caused by coal and LNG and the other 3.6% were caused by nuclear, biomass, geothermal, oil, offshore wind and solar PV. The remaining resources did not increase their output. Lastly, the BAU overall performed slightly better (99.55% demand coverage) than the transport-integrated scenario (99.31% demand coverage), suggesting that the planned future installed capacity volume is neither sufficient nor is it distributed optimally to meet the increase in demand from electrified transport. At the same time, the increase in the generation

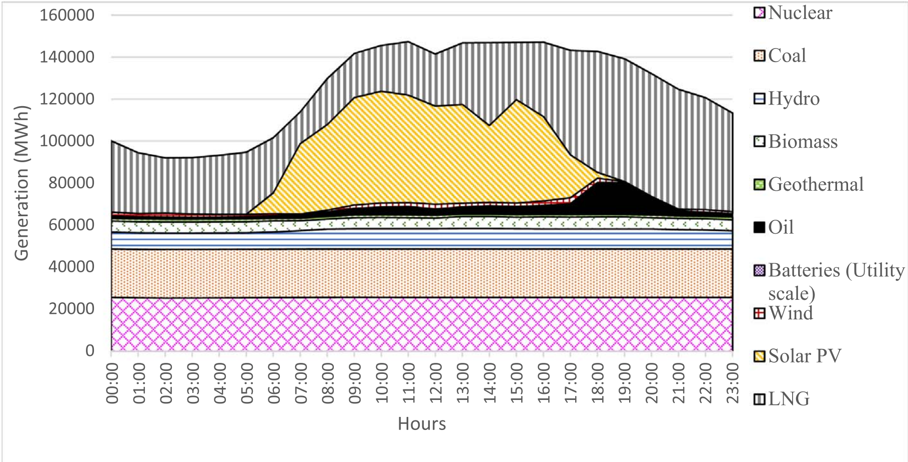

Figure 12. Hourly generation by resource (MWh) on the 9th of August.

Table 14. Total generation by resource (GWh) on the 9th of August.

Resource	Nuclear	Coal	Hydro	Biomass	Geothermal	Oil	Batteries	Wind	Solar PV	LNG
GWh	611.5	554.4	215.7	128.8	30.5	90.3	0.2	34.8	482.2	843.3
%	20.44	18.53	7.21	4.31	1.02	3.02	0.01	1.16	16.12	28.19

of all renewable sources (except onshore wind and conventional hydro) suggests that electrified transport is generally compatible with renewables, which are prioritized in the 6th SEP.

4 Discussion

The electricity demand curves for BEV and FCEV vehicles were found to be distinct from each other, which mainly stemmed from different refuelling/charging patterns. Therefore, when studying the impact of transport demand integration into the energy system, it is important to estimate the total electricity demand curve as a composite of each technology's individual demand. Compared to previous literature, the BEV electricity demand curve estimated in this study is highly day (rather than night-time) focused, due to the low availability of home chargers (10.6% of all chargers). This illustrates that the type of infrastructure available (public, workplace, private), as well as the rules around how it can be used, significantly influence the shape of the transport electricity demand curve. As some of these rules are based on legislation rather than infrastructure setup or technology, the demand curves may also differ between regions with similar infrastructure setups.

While the FCEV demand curve estimated in this study has some limitations, its morning and evening focus is likely to remain a prominent feature that sets it apart from the BEV demand curve. This also highlights that a composite transport demand curve of these two types of technologies would likely have several localised maxima throughout the day, which may in part exacerbate the current electricity demand curve at some times (*e.g.* around midday and the early evening), and even it out at others (*e.g.* the morning, when FCEVs are refuelling on the way to work). The case of the FCEV electricity demand curve also highlights the importance of explicit infrastructure modelling: the demand curve estimated in this study is based on the assumption that the HRS infrastructure electrolyses on-site and therefore FCEV demand for H_2 directly translates into instantaneous electricity demand (*i.e.* the production of H_2 using off-peak electricity and its storage for later use is not considered by the simulation). While this assumption is not unrealistic, it leaves out one of the major anticipated benefits of any H_2 network, which is the increased demand elasticity created by H_2 storage, which should be tackled by future research and improvements to the model.

Table 15. Global warming potential of each resource (gCO_2/kWhe).

Resource	gCO_2/kWhe
Nuclear (PWR)	16.95
Coal (ST)	849.64
Hydro	684.45
pumped hydro	58.41
biomass (co-generation)	54.76
geothermal	25.04
oil (HF-ST)	13.07
Utility-scale battery (li-ion)	300.00
wind (onshore)	27.55
wind (offshore)	13.00
solar PV	20.32
LNG (CC)	446.67

Table 16. Energy mix (%) comparison between BAU and the transport-integrated scenario and global warming potential.

Resource	BAU			Transport-integrated		
	mix (%)	mix (TWh)	$MtCO_2$/year	mix (%)	mix (TWh)	$MtonCO_2$/year
Nuclear	21.0	211.91	3.59	20.96	223	3.78
Coal	19.0	191.75	162.92	19.00	202	171.92
Hydro-conventional	7.97	80.43	55.05	7.39	78.70	53.86
Hydro-pumped	0.03	0.27	0.02	0.02	0.26	0.02
Biomass	4.2	42.79	2.34	4.06	43.20	2.37
Geothermal	0.9	9.37	0.23	0.90	9.53	0.24
Oil	2.8	28.25	0.37	4.00	42.60	0.56
Batteries	0.01	0.13	0.04	0.01	0.12	0.04
Wind-onshore	1.33	13.39	0.37	1.13	12.07	0.33
Wind-offshore	1.48	14.90	0.19	1.53	16.26	0.21
Solar PV	10.2	103.20	2.10	10.24	109.01	2.21
LNG	30.5	308.27	137.70	30.07	320.24	143.04
TOTAL	99.55	1004.67	364.92	99.31	1057.61	378.59

The infrastructure setup for both BEVs and FCEVs can be expected to significantly influence the shape of the transport electricity demand curve. Based on this, policy-based infrastructure development targets for both HRS and BEV chargers would be useful. However, in the case of Japan, BEV charging infrastructure development (both public and private) does not seem to have policy targets. The authors therefore recommend that transport policy should determine infrastructure development targets for both private and public BEV charger development throughout the country.

To estimate the expected electricity demand for the BAU, the transport demand share was deducted from the total estimated electricity demand (1065 TWh) estimated by METI [3]. While the government of Japan has published estimates for the number of cars and infrastructure facilities of both BEVs and FCEVs by 2030, estimated electricity demand values are less conclusive. Data related to electricity consumption often focuses on targets for the fuel economy of electrified vehicles [12, 80]. One transport electricity demand estimate for 2030 could be identified [81]: p. 73), at 190 GWh for the entire electrified fleet over a whole year. Given that, among the electrified fleet, 4.9 million BEVs are expected and given that one full charge of, for example, a Tesla model 3 requires 82 kWh, the estimated value of 190 GWh would be equivalent to less than half a full charge per BEV over the entire year. This seems highly unlikely and therefore the authors refrained from using this value in the present simulation. Instead, the authors assumed that the transport demand estimated through the model (based on the 2030 fleet and infrastructure) was representative of the 2030 transport electricity demand. It is obvious that more clarity is needed regarding how the electricity demand of various sectors (particularly transport) will be estimated in the future, given that research such as that outlined in the present paper relies heavily on such assumptions. While the authors acknowledge the limitations of the assumptions they followed when estimating the overall distribution of the transport and total electricity demand, it is also outside the scope of this paper to arrive at more accurate projections.

The demand for electricity incurred by 5.7 million BEVs and FCEVs (9.25% of all passenger vehicles expected to be on the roads of Japan by 2030) was thus estimated to comprise around 5.21% of total electricity demand by 2030. It can therefore be expected that as the electrification of the transport sector progresses, its demand share will become a significant factor when balancing the energy system. The addition of transport demand was most beneficial for solar PV and offshore wind, as well as oil, while all other resources either maintained their target shares or reduced them slightly. Two significant factors contributing to this were the country-wide spatial resource distribution and insufficient resource capacity to further increase generation. Spatial resource distribution favoured oil in particular, as regions with oil thermal generating capacity tend to be ones that also have MMAs, where the increase in demand due to the transport component was most pronounced. As electrified transport becomes more widely adopted and less concentrated in MMAs this effect might decrease.

EnSym necessarily relies on simplifying assumptions in some key areas. First, thermal power plants are assumed to run without interruption (*i.e.* no maintenance schedule is considered). Further, no thermal resource was permitted to deposit excess generation in storage (either pumped hydro or batteries). Additionally, among RES-E, only solar PV and wind resources were permitted to be deposited in storage, as geothermal and biomass capacities are highly controllable and for the most part deployed at low shares. As a result of such limitations, the available storage capacity is under-utilised. Further, all pumped hydro stations and batteries are assumed to have the same operational parameters, though this is likely to be quite varied in reality.

Second, the driver profiles (commuter and leisure) significantly rely on assumptions, as the amount of observed data is very limited. More data observations are necessary to derive a clearer picture of the different types of driving and charging behaviour, particularly for technologies with lengthy charging times. In the future, a self-driving fleet component should also be considered, as well as more profiles with more instantiations compared to the current 50.

Third, the FCEV electricity demand curve is limited by the assumption that no new infrastructure would be built between May 2021 and 2030, which means that in the simulation the HRS are constantly used, even in the middle of the night, leading to a relatively uniform curve. However, a HRS can comprise one dispenser (all current HRSs in Japan have one dispenser), or up to four, and it is likely that in the future more dispensers will be installed. Further, it is a simplification to assume that HRS infrastructure only works with on-site generation, rather than also (or even mainly) having a centralized distribution network.

Fourth, the BEV charger fleet is assumed not to be capable of vehicle-to-grid (V2G), despite this being anticipated as an important demand-side management mechanism by 2030. In terms of the impact of V2G on the current results, the authors expect that including V2G would increase the share of renewable-derived electricity from storage and decrease oil and LNG generation during the day. Further, V2G would likely increase the average number of hours per day spent connected to a charger and may increase the share of evening charging.

As a next step, vehicle to grid (V2G) and a centralized H_2 storage and distribution network should be added to the model. Further, it would be useful to differentiate private solar PV rooftops from other solar PV installations, collect observed data on driving and charging patterns of AFV owners (specific for Japan) and add partial grid outage scenarios to the simulation, addressing the potential for disaster resilience through combined energy and transport systems. Also, exploring how the relationship between energy system security, renewable integration and an AFV fleet changes as that fleet grows larger would be interesting. This would be an important benchmarking task to identify at which developmental stages renewable technology installation targets, storage, infrastructure and vehicle fleet development need to coalesce to maintain supply security while increasingly electrifying and decarbonizing the energy sector. At a more fundamental level, it is important to improve the understanding of how transport demand behaves based on different types of infrastructure and rule setups, as well as from the perspectives of a differentiated set of users, especially as new ones (*e.g.* autonomous vehicles) arise.

5 Conclusion and policy implications

The main conclusions of this work can be summarized in three points. First, the variation in electricity demand for transport throughout the day is influenced by physical infrastructure, the rules by which it can be used, technology, and how its drivers use it. Therefore, no single technology is representative of the transport electricity demand curve. To apply transport electricity demand curves from one administrative region to another, the related infrastructure, rules and driver profiles should be known, though there is scarce literature and data to inform models on this. Further, this highlights the need for more data collection that can provide specific information on these components and their daily fluctuations and geographic considerations.

Second, this study found that there is potential for symbiotic co-development between alternative fuel vehicle (AFV) infrastructure and RES-E, which is an important contribution to existing literature. However, to fully harness this potential it may be beneficial for policymakers to not only see the energy, transport and hydrogen strategies as related but instead to fully integrate them through infrastructure and resource development plans and pathways that incorporate two or all three of these strategies.

Third, this study has expanded the modelling literature by improving the EnSym model to simultaneously integrate a country-level energy system with a transmission grid and multi-technology transport sector demand. However, while the analysis conducted provides new insights into energy and transport sector developments, there are several model limitations and parameter functionality requirements that should be tackled to further improve the quality of the evaluations. It would be particularly interesting to extend the model to consider other types of vehicles, such as for example an intermediate type of vehicle, such as a utility type of FCEV. Also, the authors would like to consider transforming the current model into a Monte Carlo simulation, which should be possible given that each simulation run only takes a handful of minutes.

Acknowledgments

A part of the present work was performed as a part of activities of the Research Institute of Sustainable Future Society, Waseda Research Institute for Science and Engineering, Waseda University.

Funding

The work was financially supported by Japan Science and Technology Agency (JST) as a part of the Belmont Forum, Re-Energize DR3 project, Grant Number JPMJBF2005, and by Japan Society of Promotion of Science (JSPS) KAKENHI Grant Number JP20KK0107 and JP19K24677.

Conflicts of interest

The authors declare that all the work described in this manuscript is purely academic and that there are no conflicts of interest of any kind.

References

1 UNFCC. (2016) United Nations framework convention on climate change, in *Report of the conference of the parties on its twenty-first session, held in Paris from 30 November to 13 December 2015 (PDF)*. https://www.un.org/en/development/desa/population/migration/generalassembly/docs/globalcompact/FCCC_CP_2015_10_Add. 1.pdf/ (accessed 10.06.2019).

2 Nikkei. (2020) Suga's 2050 zero-carbon goal thrusts Japan into green tech race. Azusa Kawakami for Nikkei Asia. https://asia.nikkei.com/Spotlight/Environment/Suga-s-2050-zero-carbon-goal-thrusts-Japan-into-green-tech-race (accessed 14.11.2020).

3 Ministry of Economy, Trade and Industry (METI). (2021a) Green growth strategy through achieving carbon neutrality in 2050. https://www.meti.go.jp/english/press/2020/pdf/1225_001a.pdf (accessed: 29.04.2022).

4 Ministry of Economy, Trade and Industry (METI). (2021b) Outline of strategic energy plan. https://www.enecho.meti.go.jp/en/category/others/basic_plan/pdf/6th_outline.pdf (accessed: 12.04.2022).

5 JEPIC. (2020) *The electric power industry in Japan 2020*. Japan Electric Power Information Center, INC. https://www.jepic.or.jp/pub/pdf/epijJepic2020.pdf (accessed: 10.09.2020).

6 Ministry of Economy, Trade and Industry (METI). (2018a) 5th strategic energy plan (provisional translation). https://www.enecho.meti.go.jp/en/category/others/basic_plan/5th/pdf/strategic_energy_plan.pdf (accessed 12.04.2022).

7 Dong Y., Shimada K. (2017) Evolution from the renewable portfolio standards to feed-in tariff for the deployment of renewable energy in Japan, *Renew. Energy* **107**, 590–596.

8 Knuepfer K., Rogalski N., Knuepfer A., Esteban M., Shibayama T. (2022) A reliable energy system for Japan with merit order dispatch, high variable renewable share and no nuclear power. *Appl. Energy* (accepted).

9 REI. (2016) *Recommendations for reform of the electricity system for establishing an electricity system with a significant share of renewable energy*. Renewable Energy Institute. https://www.renewable-ei.org/en/images/pdf/20160524/DRAFT_electricity_system_reform_porposal.pdf (accessed: 17.12.2020).

10 Wakiyama T., Kuriyama A. (2018) Assessement of renewable energy expansion potential and its implications on reforming Japan's electricity system, *Energy Policy* **115** issue C, 302–316.

11 Yoshihara K., Ohashi H. (2017) *Assessing the impact of renewable energy sources: simulation analysis of the Japanese electricity market*. Research Institute of Economy, Trade and Industry. https://www.rieti.go.jp/en/publications/summary/17040014.html (accessed: 15.10.2020).

12 Ministry of Economy, Trade and Industry (METI). (2018b) Trend of next generation/zero emission vehicle and policy in Japan. Presentation from April 2018. https://www.nedo.go.jp/content/100878195.pdf (accessed: 29.04.2022).

13 Ministry of Economy, Trade and Industry (METI). (2018c) *Japan promotes electrified vehicle (xEV) strategy ahead of 2050*. Ministry of Economy, Trade and Industry. Last updated: 2018–11-20. URL: https://www.meti.go.jp/english/mobile/2018/20180911001en.html (accessed: 30.04.2022).

14 Agency for Natural Resources and Energy (ANRE). (2014) Summary of the strategic road map for hydrogen and fuel cells. https://www.meti.go.jp/english/press/2014/pdf/0624_04a.pdf (accessed: 18.06.2020).

15 Ministry of Economy, Trade and Industry (METI). (2018d) Japan H2 mobility, a company for development of hydrogen stations, established. https://www.meti.go.jp/english/press/2018/0305_001.html (accessed: 28.05.2020).

16 Ministry of Economy, Trade and Industry (METI). (2017) Basic hydrogen strategy, ministerial council on renewable energy, hydrogen and related issues (PDF). https://www.meti.go.jp/english/press/2017/pdf/1226_003b.pdf/ (accessed:12.04.2019).

17 Knüpfer K., Mäll M., Esteban M., Shibayama T. (2021) Review of mixed-technology vehicle fleet evolution and representation in modelling studies: policy contexts of Germany and Japan, *Energy Policy* **156**, 112287. https://doi.org/10.1016/j.enpol.2021.112287.

18 Mopidevi S., Narasipuram R.P., Aemalla S.R., Rajan H. (2022) E-mobility: impacts and analysis of future transportation electrification market in economic, renewable energy and infrastructure perspective, *Int. J. Powertrains* **11**, 2/3, 264–284.

19 Narasipuram R.J., Mopidevi S.A. (2021) Technological overview & design considerations for developing electric vehicle charging stations, *J. Energy Storage* **43**, 103225.

20 Solanke T.U., Ramachandaramurthy V.K., Yong J.Y., Pasupuleti J., Kasinathan P., Rajagopalan A. (2020) A review of strategic charging–discharging control of grid-connected electric vehicles, *J. Energy Storage* **28**, 101193. https://doi.org/10.1016/j.est.2020.101193.

21 Hanley E.S., Deane J.P., Gallachóir B.P.Ó. (2018) The role of hydrogen in low carbon energy futures – a review of existing perspectives, *Renew. Sustain. Energy Rev.* **82**, 3027–3045. https://doi.org/10.1016/j.rser.2017.10.034.

22 Nocera S., Cavallaro S. (2016) The competitiveness of alternative transport fuels for CO_2 emissions, *Transp. Policy* **50**, 1–14.

23 Parra D., Valverde L., Pino F.J., Patel M.K. (2019) A review of the role, cost and value of hydrogen energy systems for deep decarbonization, *Renew. Sustain. Energy Rev.* **101**, 279–294.

24 Reichmuth D.S., Lutz A.E., Manley D.K., Keller J.O. (2013) Comparison of the technical potential for hydrogen, battery electric, and conventional light-duty vehicles to reduce greenhouse gas emissions and petroleum consumption in the United States, *Int. J. Hydrog. Energy* **38**, 1200–1208.

25 Thiel C., Drossinos Y., Krause J., Harrison G., Gkatzoflias D., Donati A.V. (2016) Modelling electro-mobility: an integrated modelling platform for assessing European policies, *Transp. Res. Procedia* **14**, 2544–2553.

26 Kim M., Kim J. (2017) An integrated decision support model for design and operation of a wind-based hydrogen supply system, *Int. J. Hydrog. Energy* **42**, 3899–9915.

27 Robledo C.B., Oldenbroek V., Abbruzzese F., van Aijk A.J.M. (2018) Integrating a hydrogen fuel cell electric vehicle with vehicle-to-grid technology, photovoltaic power and a residential building, *Appl. Energy* **215**, 615–629.

28 Cao S. (2016) Comparison of the energy and environmental impact by integrating a H2 vehicle and an electric vehicle into a zero-energy building, *Energy Convers. Manag.* **123**, 153–173.

29 Das S., Panda S. (2023) An optimized fractional order cascade controller for frequency regulation of power system with renewable energies and electric vehicles, *Energy Syst.* **14**, 171–195. https://doi.org/10.1007/s12667-021-00461-9.

30 Komiyama R., Fujii Y. (2015) Assessment of energy saving and CO_2 mitigation potential of electric vehicles and plug-in hybrid vehicles under Japan's power generation mix, *Electr. Eng. Jpn.* **192**, 10–18.

31 Lee D.-H. (2014) Development and environmental impact of hydrogen supply chain in Japan: assessment by the CGE-LCA method in Japan with a discussion of the importance of biohydrogen, *Int. J. Hydrog. Energy* **39**, 19294–19310.

32 Shafiei E., Davidsdottir B., Leaver J., Stefansson H., Asgeirsson E.I. (2015) Comparative analysis of hydrogen, biofuels and electricity transitional pathways to sustainable transport in renewable-based electricity system, *Energy* **83**, 614–627.

33 Shin J., Hwang W.S., Choi H. (2019) Can hydrogen fuel vehicles be a sustainable alternative on vehicle market? Comparison of electric and hydrogen fuel cell vehicles, *Technol. Forecast Soc. Chang.* **143**, 239–248.
34 Tarroja B., Shaffer B., Samuelsen S. (2015) The importance of grid integration of achievable greenhouse gas emissions reductions from alternative vehicle technologies, *Energy* **87**, 504–519.
35 Carr S., Premier G.C., Guwy A.J., Dinsdale R.M., Maddy J. (2014) Hydrogen storage and demand to increase wind power onto electricity distribution networks, *Int. J. Hydrog. Energy* **39**, 10195–10207.
36 Hoarau Q., Perez Y. (2018) Interactions between electric mobility and photovoltaic generation: a review, *Renew. Sustain. Energy Rev.* **94**, 510–522.
37 Islam M.S., Mithulananthan N., Hung D.Q. (2019) Coordinated EV charging for correlated EV and grid loads and PV output using a novel, correlated, probabilistic model, *Int. J. Elec. Power Energy Syst.* **104**, 335–348.
38 Mwasilu F., Justo J.J., Kim E.-K., Do T.D., Jung J.W. (2014) Electric vehicles and smart grid interaction: a review on vehicle to grid and renewable energy sources integration, *Renew. Sustain. Energy Rev.* **34**, 501–516. https://doi.org/10.1016/j.rser.2014.03.031.
39 Richardson D.B. (2013) Electric vehicles and the electric grid: a review of modeling approaches, impacts, and renewable energy integration, *Renew. Sustain. Energy Rev.* **19**, 247–254.
40 Kobashi T., Yarime M. (2019) Techno-economic assessment of the residential photovoltaic systems integrated with electric vehicles: a case study of Japanese households towards 2030, *Energy Procedia* **158**, 3802–3807.
41 Mills G., MacGill I. (2018) Assessing electric vehicle storage, flexibility and distributed energy resource potential, *J. Energy Storage* **17**, 357–366.
42 Seddig K., Jochem P., Fichtner W. (2017) Integrating renewable energy sources by electric vehicle fleets under uncertainty, *Energy* **141**, 2145–2153.
43 Dodds P.E., McDowall W. (2014) Methodologies for representing the road transport sector in energy system models, *Int. J. Hydrog. Energy* **39**, 5, 2345–2358.
44 Park S., Yoo J., Han S.J., Song J.H., Lee E.J., Song I.K. (2017) Steam reforming of liquefied natural gas (LNG) for hydrogen production over nickel–boron–alumina xerogel catalyst, *Int. J. Hydrog. Energy* **42**, 22, 15096–15106.
45 Komiyama R., Fujii Y. (2017) Modeling analysis of electric vehicle penetration scenario using dynamic optimal power generation mix model with high temporal resolution, *Electr. Eng. Jpn.* **199**, 61–70.
46 Madzharov D., Delarue E., D'haeseleerW. (2014) Integrating electric vehicles as flexible load in unit commitment modeling, *Energy* **65**, 285–294.
47 Taljegard M., Göransson L., Odenberger M., Johnsson F. (2019) Impacts of electric vehicles on the electricity generation portfolio – a Scandinavian-German case study, *Appl. Energy* **235**, 1637–1650.
48 Verzijlbergh R., Martínez-Anido C.B., Lukszo Z., de Vries L. (2014) Does controlled electric vehicle charging substitute cross-border transmission capacity?, *Appl. Energy* **120**, 169–180.
49 Iacobucci R., McLellan B., Tezuka T. (2018a) Modeling shared autonomous electric vehicles: potential for transport and power grid integration, *Energy* **158**, 148–163.
50 Iacobucci R., McLellan B., Tezuka T. (2018b) The synergies of shared autonomous electric vehicles with renewable energy in a virtual power plant and microgrid, *Energies* **11**, 2016.
51 Kroog Ekman C. (2011) On the synergy between large electric vehicle fleet and high wind penetration – an analysis of the Danish case, *Renew. Energy* **36**, 2, 546–553.
52 Lund H., Kempton W. (2008) Integration of renewable energy into the transport and electricity sectors through V2G, *Energy Policy* **36**, 9, 3578–3587.
53 Cutter E., Conlon B., Garnett O., Zhang J., Ryan N. (2019) California framework for grid value of vehicle grid integration (VGI): presentation to VGI working group on 12th April 2019. https://gridworks.org/wp-content/uploads/2019/05/VGI_4.12-Slides.pdf (accessed: 20.05.2021).
54 Ramesh R. (2021) Assembly bill 2127 electric vehicle charging infrastructure assessment: staff report. Docket number: 19-AB-2127.
55 Felgenhauer M.F., Pellow M.A., Benson S.M., Hamacher T. (2016a) Economic and environmental prospects of battery and fuel cell vehicles for the energy transition in German communities, *Energy Procedia* **99**, 380–391.
56 Felgenhauer M.F., Pellow M.A., Benson S.M., Hamacher T. (2016b) Evaluating co-benefits of battery and fuel cell vehicles in a community in California, *Energy* **114**, 360–368.
57 Zhang Q., McLellan B.C., Tezuka T., Ishihara K.N. (2013) An integrated model for long-term power generation planning toward future smart electricity systems, *Appl. Energy* **112**, 1424–1437.
58 McPherson M., Karney B. (2017) A scenario based approach to designing electricity grids with high variable renewable energy penetrations in Ontario, Canada: development and application of the SILVER model, *Energy* **138**, 185–196.
59 Moliner R., Lazaro M.J., Suelves I. (2016) Analysis of the strategies for bridging the gap towards the hydrogen economy, *Int. J. Hydrog. Energy* **41**, 19500–19508.
60 Ministry of Economy, Trade and Industry (METI). (2021c) 2030 年における再生可能エネルギーについて(transl.: About renewable energy in 2030). https://www.meti.go.jp/shingikai/enecho/denryoku_gas/saisei_kano/pdf/031_02_00.pdf (accessed: 29.06.2022).
61 OCCTO. (2019) Aggregation of electricity supply plans, fiscal year 2019. Figure 3–6: composition of installed power generation capacity for each regional service area. p. 24. http://www.occto.or.jp/en/information_disclosure/supply_plan/files/supplyplan_2019.pdf (accessed: 15.10.2020).
62 FiT. (2022) 固定価格買取制度 情報公表用ウェブサイト ("Feed-in tariff website for information disclosure"). https://www.fit-portal.go.jp/PublicInfoSummary (accessed: 12.04.2022).
63 Chen Y.T., Knuepfer K., Esteban M., Shibayama T. (currently under review) *Renewable Energy*.
64 DOE Global Energy Storage Database. (2020) Global energy database projects 21–09-2020: battery_cap-01-2020.01.04. https://www.sandia.gov/ess-ssl/global-energy-storage-database-home/ (accessed: 18.10.2020).
65 JMA. (2020) 過去の気象データ·ダウンロード(Past meteorological data download landing page). Japan Meteorological Agency. https://www.data.jma.go.jp/gmd/risk/obsdl/index.php (accessed: 19.12.2020).
66 Agency for Natural Resources and Energy (ANRE). (2020) 電力調査統計表 過去のデータ: Table 2-(2) of each relevant year. https://www.enecho.meti.go.jp/statistics/electric_power/ep002/results_archive.html (accessed: 20.10.2020).

67 TEPCO. (2020) Hourly demand progression. http://www.tepco.co.jp/en/forecast/html/download-e.html (accessed: 03.08.2020).
68 NeV. (2018) 都道府県別補助金交付状況 充電設備 ("Subsidy grant status by prefecture for charging equipment"). http://www.cev-pc.or.jp/tokei/koufu3.html (accessed: 20.05.2021).
69 Sun X. (2016) Charging behavior of battery electric vehicle users in Japan. Doctoral Dissertation: Nagoya University. http://hdl.handle.net/2237/24286. https://nagoya.repo.nii.ac.jp/?action=pages_view_main&active_action=repository_view_main_item_detail&item_id=22078&item_no=1&page_id= 28&block_id=27 (accessed: 5.7.2020).
70 IPSS. (2020) Table 1. Total population by municipality in Japan: 2015–2045. National Institute of Population and Social Security Research. http://www.ipss.go.jp/pp-shicyoson18/t-page.asp (accessed 19.10.2020).
71 Stat. (2013). *Table 21–3: Dwellings by type of dwelling, type of building, stories of building and prefecture (1988–2013)*. Housing and Land Survey.
72 CEV. (2021) FCEV number of HRS and location. http://www.cev-pc.or.jp/suiso_station/index.html (accessed: 18.07.2020).
73 JHyM. (2020) Japan H2 mobility. About JHyM. https://www.jhym.co.jp/en/nav-about/ (accessed 14.11.2020).
74 Statista. (2019) Number of gasoline filling stations in Japan from 2002 to 2018. https://www.statista.com/statistics/870206/japan-number-gas-stations/ (accessed 14.11.2020).
75 KBA. (2021) Jahresbilanz – Bestand. https://www.kba.de/DE/Statistik/Fahrzeuge/Jahresbilanz/bestand_jahresbilanz_node.html (accessed: 04.05.2021).
76 Pareschi G., Küng L., Georges G., Boulouchos K. (2020) Are travel surveys a good basis for EV models? Validation of simulated charging profiles against empirical data, *Appl. Energy* **275**, 115318.
77 Rapier R. (2020) Estimating the carbon footprint of utility-scale battery storage. Forbes. https://www.forbes.com/sites/rrapier/2020/02/16/estimating-the-carbon-footprint-of-utility-scale-battery-storage/?sh=2ef247407adb (accessed: 06.06.2021).
78 House of Parliament. (2011) parliament.uk/globalassets/documents/post/postpn_383-carbon-footprint-electricity-generation.pdf (accessed: 20.04.2022).
79 Portugal-Pereira J., Esteban M. (2014) Implications of paradigm shift in Japan's electricity security of supply: a multi-dimensional indicator assessment, *Appl. Energy* **123**, issue C, 424–434.
80 Ministry of Economy, Trade and Industry (METI). (2021d) Japan's energy 2020. https://www.enecho.meti.go.jp/en/category/brochures/pdf/japan_energy_2020.pdf (accessed: 29.06.2022).
81 Ministry of Economy, Trade and Industry (METI). (2021e) 2030 年度におけるエネルギー需給の見通し（関連資料）(transl.: Outlook for energy supply and demand in 2030 (related materials)). https://www.enecho.meti.go.jp/committee/council/basic_policy_subcommittee/opinion/data/03.pdf (accessed: 29.06.2022).
82 JAIF. (2019) Current status of nuclear power plants in Japan. https://www.jaif.or.jp/cms_admin/wp-content/uploads/2019/09/jp-npps-operation20190905_en.pdf (accessed: 29.06.2022).
83 NEV. (2020) 水素ステーション設備状況 ("Hydrogen station facilities"). http://www.cev-pc.or.jp/suiso_station/index.html (accessed: 13.04.2022).
84 IEA. (2015) Large-scale hydrogen delivery infrastructure: final report, *Expert Group Task 28. International Energy Agency, Hydrogen Implementing Agreement*. ISBN 978-0-9815041-8-6. URL: https://www.ieahydrogen.org/tasks-reports/ (accessed: 04.05.2021).
85 IRENA. (2020) *Green Hydrogen Cost Reduction: scaling up electrolysers to meet the 1.5C Climate Goal*, International Renewable Agency, Abu Dhabi. https://irena.org/-/media/Files/IRENA/Agency/Publication/2020/Dec/IRENA_-Green_hydrogen_cost_2020.pdf (accessed: 25.04.2021).
86 J-POWER. (2022). Geothermal power generation business. https://www.jpower.co.jp/bs/renewable_energy/geothermal/ (accessed: 12.04.2022).
87 J-POWER. (2019a) Construction works started at Appi Geothermal Power Plant. https://www.jpower.co.jp/english/news_release/pdf/news190910.pdf (accessed: 12.04.2022).
88 J-POWER. (2019b) Onikoube power plant. https://www.jpower.co.jp/english/news_release/pdf/news190910.pdf (accessed: 12.04.2022).
89 EPA. (2018a) 2018 Nissan Leaf compare side-by-side. US Department of Energy, U.S. Environmental Protection Agency. https://www.fueleconomy.gov/feg/Find.do?action=sbs&id=39860 (accessed: 04.05.2021).
90 EPA. (2018b) 2018 Tesla Model 3 Long Range compare side-by-side. US Department of Energy, U.S. Environmental Protection Agency. https://www.fueleconomy.gov/feg/Find.do?action=sbs&id=39836 (accessed: 04.05.2021).
91 Kane M. (2014) Toyota Mirai fuel cell Sedan priced at $57,500 – specs, videos. Article for InsideEVs. https://insideevs.com/news/323973/toyota-mirai-fuel-cell-sedan-priced-at-57500-specs-videos/ (accessed: 29.06.2022).

Appendix

Nuclear power target capacity adjustment

The nuclear capacity in the model was reduced from the expected 38.04 [4] to 33.2 GW. The reported installed nuclear capacity in 2018 [61] includes 4.4 GW installed at Fukushima Daiichi and Daini, which have since been completely scrapped [82]. A further 810 MW capacity has been removed, as is not listed in the annual status update provided by the Japan Atomic Industrial Forum [82], and it is therefore unclear where that capacity would come from. Further, 8.2 GW of TEPCO-owned capacity is assigned to Hokuriku, as this is the region where it is located in. While 6.5 GW of Kansai's capacity is located in Hokuriku, these power stations connect to the Kansai regional grid directly and are therefore assigned to Kansai. Table A1 provides an overview of all nuclear power plants considered.

Geothermal regional capacity development projects leading up to 2030

By 2030, five geothermal plants totalling 66.1 MW are scheduled to connect to the energy grid (Table A2). Given the 500 MW already installed in 2022, the total, regionally distinguishable installed capacity for geothermal is 566.1 MW. The remaining 933.9 MW scheduled to go online by 2030 were distributed over the regions proportionately.

Table A1. Installed nuclear capacity (MW) assumed to be available in 2030 by region, based on the installed operational capacity in 2018 (Source: [82]).

Plant name	Owner	Location	Capacity
TOKAI-2	JAPC	Kanto	1100
TSURUGA-2	JAPC	Hokuriku	1160
TOMARI-1	Hokkaido EPC	Hokkaido	579
TOMARI-2	Hokkaido EPC	Hokkaido	579
TOMARI-3	Hokkaido EPC	Hokkaido	912
ONAGAWA-2	Tohoku EPC	Tohoku	825
ONAGAWA-3	Tohoku EPC	Tohoku	825
HIGASHIDORI-1	Tohoku EPC	Tohoku	1100
KASHIWAZAKI KARIWA-1	TEPCO	Hokuriku	1100
KASHIWAZAKI KARIWA-2	TEPCO	Hokuriku	1100
KASHIWAZAKI KARIWA-3	TEPCO	Hokuriku	1100
KASHIWAZAKI KARIWA-4	TEPCO	Hokuriku	1100
KASHIWAZAKI KARIWA-5	TEPCO	Hokuriku	1100
KASHIWAZAKI KARIWA-6	TEPCO	Hokuriku	1356
KASHIWAZAKI KARIWA-7	TEPCO	Hokuriku	1356
HAMAOKA-3	Chubu EPC	Chubu	1100
HAMAOKA-4	Chubu EPC	Chubu	1137
HAMAOKA-5	Chubu EPC	Chubu	1380
SHIKA-1	Hokuriku EPC	Hokuriku	540
SHIKA-2	Hokuriku EPC	Hokuriku	1358
MIHAMA-3	Kansai EPC	Hokuriku	826
TAKAHAMA-1	Kansai EPC	Hokuriku	826
TAKAHAMA-2	Kansai EPC	Hokuriku	826
TAKAHAMA-3	Kansai EPC	Hokuriku	870
TAKAHAMA-4	Kansai EPC	Hokuriku	870
OHI-3	Kansai EPC	Hokuriku	1180
OHI-4	Kansai EPC	Hokuriku	1180
SHIMANE-2	Chugoku EPC	Chugoku	820
IKATA-3	Shikoku EPC	Shikoku	890
GENKAI-3	Kyushu EPC	Kyushu	1180
GENKAI-4	Kyushu EPC	Kyushu	1180
SENDAI-1	Kyushu EPC	Kyushu	890
SENDAI-2	Kyushu EPC	Kyushu	890
Total operable capacity:			33,235

Table A2. Geothermal power plants currently under construction or refurbishment [60, 86–88].

Project name	Region	Planned capacity (MW)	Planned start date	Developer
Minamikayabe	Hokkaido	6.5	2022	FIT
Onikoube	Tohoku	14.9	2023	JPOWER
Appi	Tohoku	14.9	2024	JPOWER
Oyasu	Tohoku	14.9	2026	FIT
Kijiyama	Tohoku	14.9	2029	FIT

Solar PV and wind data measurement stations

Table A3 lists the weather stations used to measure solar PV, onshore wind, and offshore wind potential generation [65].

BEV charging infrastructure makeup and distribution

The total BEV charging infrastructure by prefecture for 2030 $\left[N_{I,BEV,pref,2030}\right]$, including public and private chargers, is given as:

$$N_{I,BEV,pref,2030} = N_{I,BEV,pref,2018} \times \left(\frac{N_{I,BEV,\,total,2030}}{N_{I,BEV,total,2018}}\right) \tag{A1}$$

Where *pref* denotes each prefecture.

The regional distribution of BEV charging infrastructure by region $\left[N_{I,BEV,region,2030}\right]$ is given by the sum of chargers in each prefecture that constitutes a region:

$$N_{I,\,BEV,\,region,\,2030} = \sum \left(N_{I,BEV,pref,2030}\right) \tag{A2}$$

It was assumed that the current infrastructure distribution will be representative of 2030, based on the data provided by NEV [68].

The number of chargers located in each city $\left[N_{I,BEV,city,2030}\right]$ is given as:

$$N_{I,BEV,city,2030} = N_{I,\,BEV,pref,2030} \times \left(\frac{P_{city,2018}}{P_{pref,2018}}\right) \tag{A3}$$

Where P denotes the human population of a location. The population by city of each city is provided by IPSS [70]. The total number of chargers located in an MMA $[N_{I,\,BEV,\,MMA,\,2030}]$ is given by the sum of the chargers located in the cities that comprise each MMA.

$$N_{I,\,BEV,\,MMA,\,2030} = \sum \left(N_{I,BEV,city,2030}\right) \tag{A4}$$

Lastly, the number of private chargers in each prefecture $\left[N_{I,BEV,pr,pref,2030}\right]$ is given as:

$$N_{I,BEV,pr,\,prefecture,2030} = N_{I,BEV,pref,2030} \times c_{pr} \tag{A5}$$

where c_{pr} denotes a constant for the share of private chargers, which takes a value of 10.6% [69].

The number of private chargers located in each city $\left[N_{I,BEV,pr,city,2030}\right]$ is given as:

$$N_{I,BEV,pr,city,2030} = N_{I,BEV,pr,pref,2030} \times \left(\frac{hd_{d,city,2018}}{hd_{d,pref,2018}}\right) \tag{A6}$$

where hd_d denotes detached households, which are provided at the city-level by Stat [71].

The number of private chargers located in an MMA $[N_{I,\,BEV,\,pr,MMA,\,2030}]$ is given as the sum of private chargers located in the cities comprising each MMA:

$$N_{I,\,BEV,\,pr,MMA,\,2030} = \sum \left(N_{I,BEV,pr,city,2030}\right) \tag{A7}$$

Table A3. List of chosen JMA station IDs by prefecture and resource (Source: [65]).

Prefecture	Wind onshore	Wind offshore	Solar PV
Hokkaido	s47420	24101	a0047
Aomori	a1122	–	s47581
Akita	a0186	32616	a0183
Iwate	a0211	–	a0236
Yamagata	a1465	–	s47520
Miyagi	a1626	–	s47590
Fukushima	s47570	–	a1034
Tochigi	s47615	–	a0335
Ibaraki	s47629	–	s47629
Saitama	s47626	–	s47626
Gunma	s47624	–	a1021
Chiba	s47648	–	a0376
Tokyo	a0371	44226	a0370
Kanagawa	a0392	–	a1443
Yamanashi	s47638	–	a1023
Shizuoka	s47655	50506	a0451
Niigata	a1469	54166	s47604
Nagano	a0399	–	a0399
Toyama	a1533	–	s47606
Fukui	a1071	–	s47616
Ishikawa	s47600	–	s47605
Gifu	a0493	–	s47632
Mie	a1230	–	a0509
Aichi	a0470	–	a0984
Shiga	a0586	–	a0963
Nara	a0635	–	s47780
Wakayama	a1485	65036	s47778
Osaka	a1471	–	s47772
Kyoto	s47750	–	s47750
Hyogo	s47776	–	s47770
Kagawa	s47891	–	s47891
Tokushima	s47895	–	a1242
Kochi	s47898	74271	a1249
Ehime	a1456	–	a0739
Tottori	a1519	–	a1231
Shimane	s47755	–	a0704
Okayama	s47768	–	a0668
Hiroshima	a0686	67511	a0686
Yamaguchi	a0779	–	a0775
Fukuoka	a0943	–	a0943
Saga	a1610	–	a0829
Kumamoto	a1240	–	a0834
Nagasaki	s47805	84072	a0922
Oita	s47814	–	a1237
Miyazaki	s47822	87492	s47822
Kagoshima	a0895	–	s47827

Table A4. BEV vehicle model specifications [89, 90].

Parameter	Unit	Nissan Leaf II	Tesla Model 3
Battery rated capacity	kWh	40	62
Charging duration	h	6.06	normal = 9.39 fast = 0.32
Max allowable depth of discharge	%	90	90
Range (nominal)	km	243	425
Usage	kWh/100 km	21.2	17
Charging power (*i.e.* plug)	kW	6.6 for non-V2G	≤200 (only on fast charger) 6.6 assumed otherwise.

Table A5. FCEV vehicle model specifications (Source: [91]).

Parameter	Unit	Toyota Mirai
Tank capacity	kg	5
Range	Km	502
Fuel efficiency	mpge	67
Output density	kW/L	3.1
Refuelling time	Minutes	3–5
FC stack max output	kW	114
Min. fill at time of charging event	%	95

Table A6. Weighted daily driving range distribution for AFVs.

Weight	driving range
0.29	10–13
0.27	13.1–21.9
0.18	22–30.6
0.18	30.7–52.6
0.06	52.7–87.6
0.02	87.7–180

Drivetrain specifications for each car model

Tables A4 and A5 summarize the parameters used for the representative BEV and FCEV vehicles, respectively.

AFV fleet distribution by region and MMA

The number and distribution of BEVs and FCEVs purchased with subsidies as of 2018 are provided by NEV [68]. The distribution factor of AFVs purchased through the subsidy scheme by prefecture $\left[\Gamma_{cars,sub,pref,2018}\right]$ is given as:

$$\Gamma_{cars,sub,pref,2018} = \frac{N_{cars,sub,pref,2018}}{N_{cars,sub,total,2018}} \tag{A8}$$

The distribution factor provided by equation (A8) is assumed to be representative of the entire fleet for each of these technologies, and it is also assumed that demographic changes will not affect the average number of vehicles per 100 households in each prefecture. Provided these assumptions hold, the distribution of the 2018 fleet for each AFV technology by prefecture $\left[N_{cars,pref,2018}\right]$ can be estimated by:

$$N_{cars,pref,2018} = N_{cars,total,2018} \times \Gamma_{cars,sub,pref,2018} \tag{A9}$$

where $N_{cars,total,2018}$ denotes the total number of AFVs in each fleet, which is provided by METI [12].

Based on the 2018 fleet of each technology, the 2030 fleets by prefecture $\left[N_{cars,pref,2030}\right]$ can be estimated as:

$$N_{cars,pref,2030} = N_{cars,total,2030} \times \Gamma_{cars,sub,pref,2018} \tag{A10}$$

To estimate the distribution of vehicles between MMAs and the rest of each region, it is assumed that the distribution of each technology's refuelling/charging infrastructure is also representative of the vehicle distribution. The number of AFVs of each technology in each city $\left[N_{cars,city,2030}\right]$ is given as:

$$N_{cars,city,2030} = N_{cars,pref,2030} \times \left(\frac{N_{I,cars,city,2030}}{N_{I,cars,pref,2030}}\right) \tag{A11}$$

Where $N_{I,cars}$ denotes the number of chargers or HRS for each technology.

The number of AFVs of each technology in each MMA by 2030 $[N_{cars,MMA,2030}]$ is given by the sum of the number of cars for each technology in the cities comprising the MMA:

Table A7. The driver profile.

Variable	Unit	Permissible value range	Description
Driver type	–	–	The driver type is an individualized instantiation of the abstract driver profile. It provides a range of values for each parameter. In this work, a "commuter" and "leisure" profiles were defined.
Daily driving distance	km	0–180 km (Toyota) 0–196 km (Tesla) 0–143 (Nissan)	This distance is covered on the days of the week that the driver profile specified (otherwise every day) and is split evenly over two trips (leaving home and returning home). The assumed boundary range is given for each vehicle technology based on its average fuel consumption and legal speed limits (max. 90 km/h in Japan). The simulation sets the average daily driving distance across the fleet according to Sun [69].
Driving hours	HH:mm–HH:mm	00:00–23:00	This refers to the specific period in which a car should be moving at an average speed so that the planned distance can be covered. During this period, an FCEV may decide to refuel but a BEV cannot decide to charge. For one trip the starting time must be earlier than the finish time. Further, the first trip of the day must end before the second trip begins.
Parking hours	HH:mm–HH:mm	00:00–23:00	This refers to non-moving periods that are not at home. These are automatically assigned to follow the first driving time of the day and to end when the second driving time begins. Home chargers cannot be accessed during this period.
Home hours	HH:mm–HH:mm	00:00–23:00	This refers to non-moving times when the vehicle is at home. These are automatically assigned to follow the last driving time of the day and to end when the first driving time of the next day begins. Any type of charger can be accessed during this period.
Driving hours flexibility	HH:mm–HH:mm	±2 on weekdays ±3 on weekends	This refers to the permissible variability in driving times between subsets. That is, if the driving time is set to start at 8:00 with a permissible flexibility of 2 h, then the driving time of any subset could start between 6:00–10:00.
Minimum want charge	%	0–100	This refers to the minimum fill level that the battery or tank has to reach for the driver to begin requesting a charger/HRS connection. If the attempt is unsuccessful, the driver will request again the next hour but not queue.
Minimum must charge	%	0–100	This refers to the minimum fill level that the battery or tank has to reach for the driver to queue after an unsuccessful charger/HRS connection request.
Driver type spatial split (MMA/rest of region)	Ratio MMA : rest of region	0:10	This refers to whether and how much bias for a specific driver type there should be between metropolitan areas and the rest of each region. For instance, at a 0:10 ratio for a driver profile, that profile would be completely absent from MMAs.

Table A8. FCEV driver profile patterns and number of subsets (N) of each profile pattern.

Parameter	Unit	Commuter ($N = 24$)	Leisure ($N = 24$)
Average daily driving distance	km/day	25.7–27	24.4–25.7
Weekday driving hours	Hh:mm–hh:mm		
Leave home		08:00–09:00	16:00–17:00
Return home		17:00–18:00	20:00–21:00
Weekend driving hours	Hh:mm–hh:mm		
Leave home		10:00–11:00	08:00–09:00
Return home		15:00–16:00	20:00–21:00
Parking hours	Hh:mm–hh:mm		
Weekday		09:00–17:00	17:00–20:00
Weekend		11:00–15:00	09:00–20:00
Home hours	Hh:mm–hh:mm		
Weekday		18:00–08:00	21:00–16:00
Weekend		16:00–10:00	21:00–08:00
Driving hours flexibility	hours		
Weekday		2	2
Weekend		3	3
Minimum want refuel	%	30	30
Minimum must refuel	%	10	10
Driver type spatial split	MMA : rest of region	2:8	6:4

Table A9. BEV driver profile patterns and number of subsets (N) of each profile patterns.

Parameter	Unit	Commuter ($N = 25$)	Leisure ($N = 25$)
Average daily driving distance	km/day	25.7–27	24.4–25.7
Weekday driving hours	Hh:mm–hh:mm		
Leave home		08:00–09:00	16:00–17:00
Return home		17:00–18:00	20:00–21:00
Weekend driving hours	Hh:mm–hh:mm		
Leave home		10:00–11:00	08:00–09:00
Return home		15:00–16:00	20:00–21:00
Parking hours	Hh:mm–hh:mm		
Weekday		09:00–17:00	17:00–20:00
Weekend		11:00–15:00	09:00–20:00
Home hours	Hh:mm–hh:mm		
Weekday		18:00–08:00	21:00–16:00
Weekend		16:00–10:00	21:00–08:00
Driving hours flexibility	hours		
Weekday		2	2
Weekend		3	3
Minimum want refuel	%	15	15
Minimum must refuel	%	10	10
Driver type spatial split	MMA : rest of region	2:8	6:4

Table A10. Infrastructure use rules for BEV chargers and FCEV hydrogen refuelling stations (HRS).

Rule	Charger	HRS
Charging/refuelling procedure	• Generally, connection is made on first-come first-serve basis. • Both home and public chargers will automatically disconnect when the battery is full. • Additionally, public charger connection time ≤8 h, irrespective of the battery charge state. After this time, the BEV will disconnect.	• If an FCEV is allotted a dispenser during an hour, it will complete the refuelling procedure within that hour. • Irrespective of the tank level, refuelling is assumed to require 5 minutes.
Infrastructure preference	• Those with home chargers can use either home or public infrastructure but will prefer home chargers. • Those without home chargers only have access to public chargers. • Among public chargers, all BEVs will prefer the fastest plugs available. • No cross-regional charging possible.	• No cross-regional refuelling possible. • No preference within a region.
Queueing	• If the number of connection requests exceeds the number of available chargers/HRS in a region, then those that are immediately connected are randomly chosen from the pool of requests. • Those that requested connecting to chargers/HRS, and that cannot connect during a given hour, and that **are not** at a critical charge/tank level, will continue their activities and request connection again in the next hour (no queueing). • Those that requested connecting to chargers/HRS, and that cannot connect during this hour, and that **are** at a critical charge/tank level, will queue in random order during this hour. They wait as many consecutive hours as necessary to recharge/refuel as necessary.	
Reconnection intervals	• If a BEV disconnects from a public charger at time t, then the next time it can request reconnection is t+2.	• None. Can immediately request reconnection if necessary.
Movement delay	• Any scheduled movement (commuting from home, parking during the day, commuting home, parking at home) can be delayed if the vehicle is queueing. • Once the charging/refuelling procedure is complete after queueing and delaying movement, the scheduled movement is carried out. • If the movement plan is delayed at any point during the day, this may cause the delay of subsequent movement plans over the same day. To avoid a permanent spillover effect on the next day, the movement plan is reset by the first commute of the next day.	

$$N_{cars,MMA,2030} = \sum \left(N_{cars,city,2030}\right) \quad \text{(A12)}$$

Driver behaviour parameters

The daily driving distance $\left[d_d\left(\frac{km}{day}\right)\right]$ is constrained by:

$$d_{min} \leq \ d_d \leq (d_t \times v_{max}) \quad \text{(A13)}$$

where d_{min} denotes the minimum daily driving distance $\left[\frac{km}{day}\right]$, which takes a value of 10, and d_t denotes the driving duration $\left[\frac{h}{day}\right]$, which takes a value of 2 for both the commuter and leisure profiles in this study. Lastly, v_{max} denotes the typical speed limit $\left[\frac{km}{h}\right]$ on Japanese highways, which takes a value of 90.

The actual daily distance is estimated considering two things: first, a weighted driving range distribution was created (Table A6), accounting for the driving distance distributions observed by Sun [69].

The driver profile

Table A7 provides the driver profile generated for each driver, together with a description of each variable and its permissible range and unit.

Tables A8 and A9 provide the setups for each driver type ("commuter" and "leisure") adopted in the present study.

Infrastructure use rules

Note that the definitions for queueing and movement delay apply to BEVs and FCEVs equally (Table A10).

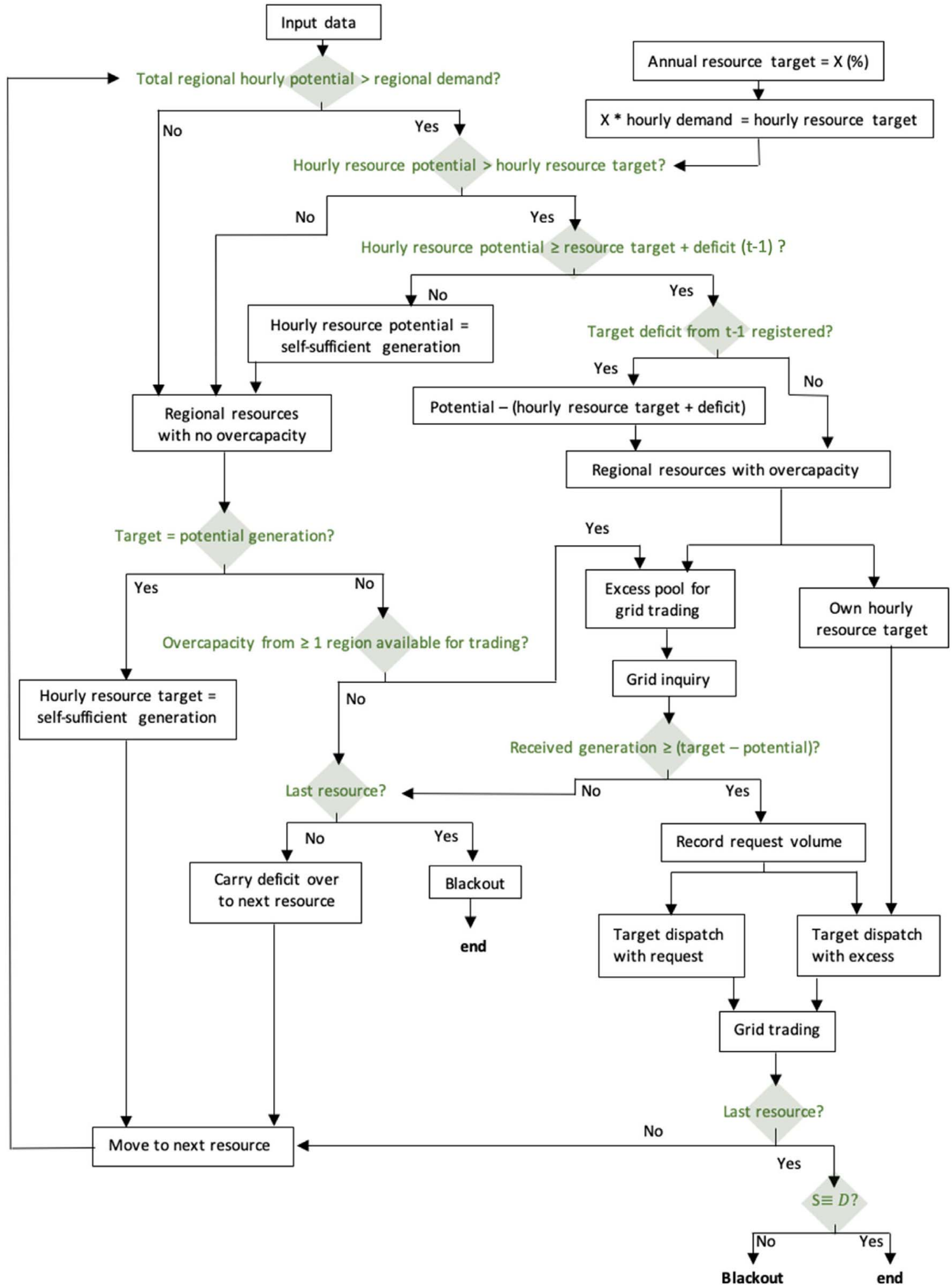

Figure A1. EnSym balancing workflow for one hour and one resource in one region.

Simulation workflow of EnSym

The main simulation workflow of EnSym is summarised in Figure A1 (see [8]), which indicates the balancing procedure for each resource, in each region, for each hour. The workflow can be divided into the following tasks:

1. Regional estimation of available capacity (or whether a capacity deficit exists at a given hour) by resource,
2. Hourly resource target setting.
3. Estimation of excess capacity or deficits in a given hour that can be traded between regions depending on grid constraints.
4. Aggregation and tabulation of results for all regions.